THE JOURNAL OF COMPARATIVE NEUROLOGY 411:327–345 (1999)

Pattern Formation by Retinal Afferents in the Ferret Lateral Geniculate Nucleus: Developmental Segregation and the Role of N-Methyl-D-Aspartate Receptors

JONG-ON HAHM, KARINA S. CRAMER, AND MRIGANKA SUR*
Department of Brain and Cognitive Sciences, Massachusetts Institute of Technology, Cambridge, Massachusetts 02139

ABSTRACT

The projection from the retina to the lateral geniculate nucleus (LGN) in ferrets segregates during development into eye-specific layers and ON/OFF sublayers. The projection pattern and the morphology of single axons was examined at several postnatal ages. The axons progress from a simple, sparsely branched morphology at birth to crude arbors at postnatal day 7 (P7). At P14–P15, axons have terminal arbors that span one eye-specific layer. By P19–P21, retinal afferents in the A layers have segregated into inner and outer sublaminae that correspond to ON- and OFF-center cells. Sublaminae form mainly by directed growth of terminal arbors in appropriately positioned regions of the LGN, along with elimination of extraneous branches in inappropriate regions. From P28 to P35, the LGN assumes an adult-like shape, and retinogeniculate axons form terminal boutons on branch endings. During the period between P14 and P21, when retinogeniculate axons segregate into ON/OFF sublaminae, N-methyl-D-aspartate (NMDA) receptors were blocked with chronic infusion of specific antagonists into the LGN. NMDA receptor blockade prevents the retinal afferent segregation into ON/OFF sublaminae. Some individual retinogeniculate axons have arbors that are not restricted appropriately, and most are restricted in size but are located inappropriately within the eye-specific laminae. Thus, NMDA receptor blockade prevents the positioning of retinogeniculate arbors that lead to the formation of ON/OFF sublaminae in the LGN. These results indicate that the activity of postsynaptic cells, and the activation of NMDA receptors in particular, can influence significantly the patterning of inputs and the structure of presynaptic afferents during development. J. Comp. Neurol. 411:327–345, 1999.

Indexing terms: axonal arborization; activity-dependent segregation; N-methyl-D-aspartate receptor blockade; ON-center cells; OFF-center cells

Specific connectivity in the mammalian retinogeniculate projection develops through a segregation process in which afferents from the two eyes in the lateral geniculate nucleus (LGN) gradually sort from an overlapped state into layers or laminae corresponding to input from one eye (Rakic, 1979; Linden et al., 1981; Bunt et al., 1983; Shatz, 1983; Cucchiaro and Guillery, 1984). In mustelids, such as ferrets and minks, the visual pathway is stratified further, in that inputs from ON-center and OFF-center retinal ganglion cells also are segregated within eye-specific layers in the lateral geniculate nucleus (LeVay and McConnell, 1982; Stryker and Zahs, 1983; Roe et al., 1989). The anatomic segregation of ON and OFF afferents occurs some time after eye-specific segregation is complete (Linden et al., 1981).

The disruption of afferent activity (for example, by suturing the lids of one eye) has been found to cause a host

Grant sponsor: National Institutes of Health; Grant numbers: EY07023 and EY11512.

Jong-On Hahm's current address is: Department of Neurosurgery, Georgetown University Medical Center, Washington, DC 20007.

Karina S. Cramer's current address is: Virginia Merrill Bloedel Hearing Research Center, Department of Otolaryngology and Head and Neck Surgery, University of Washington, Seattle, WA 98195.

*Correspondence to: Mriganka Sur, Department of Brain and Cognitive Sciences, Massachusetts Institute of Technology, E25–235, Cambridge, MA 02139. E-mail: msur@ai.mit.edu

Received 25 July 1997; Revised 27 January 1999; Accepted 26 March 1999

of morphologic and physiological changes in both the LGN and the visual cortex (for reviews, see Movshon and Van Sluyters, 1981; Sherman and Spear, 1982). Monocular deprivation also leads to changes in the pattern of connections at the level of the retinogeniculate synapse (Sherman, 1985; Garraghty and Sur, 1993) that have been shown to result from altered morphology of retinal ganglion cell axon arbors projecting to the LGN (Sur et al., 1982).

Because retinal ganglion cells fire spontaneous action potentials even in the absence of visual stimulation, monocular deprivation experiments only partly address the role of impulse activity. Blockade of sodium channels with tetrodotoxin (TTX) injected either into the eye or directly into the brain causes abnormal visual responses in LGN cells (Archer et al., 1982; Dubin et al., 1986) and prevents normal segregation of retinogeniculate afferents and development of retinal axon terminal arbors (Sur et al., 1985; Shatz and Stryker, 1988; Sretavan et al., 1988; Cramer and Sur, 1997). Binocular TTX treatment prevents the formation of ocular dominance columns within the primary visual cortex of cats (Stryker and Harris, 1986) and blocks the formation of ocular dominance stripes in optic tecta of frogs with a supernumerary eye (Reh and Constantine-Paton, 1985). Recently, it has been shown that blocking waves of retinal action potentials by cholinergic agents alters eye-specific segregation of retinal afferents in the LGN (Penn et al., 1998).

N-methyl-D-aspartate (NMDA) receptors have attracted attention as mediators of activity-dependent development due to their ability to detect correlated activity and their ability to flux Ca^{2+}, which can act as an intracellular catalyst of development (for reviews, see Cramer and Sur, 1995; Constantine-Paton and Cline, 1998; Cramer et al., 1998). The role of NMDA receptors in activity-dependent development of visual connections has been demonstrated in both mammalian visual cortex (Kleinschmidt et al., 1987; Bear et al., 1990) and amphibian optic tectum (Cline et al., 1987; Scherer and Udin, 1989; Cline and Constantine-Paton, 1990). NMDA receptors also mediate synaptic transmission in the LGN (Sillito et al., 1990a,b; Heggelund and Hartveit, 1990; Kwon et al., 1991) and the visual cortex (Miller et al., 1989; Fox et al., 1989). More generally, the studies mentioned above suggest that both afferent activity and target activity are required for normal development and, furthermore, that target activity can have a significant influence on the structure and function of afferents.

The present study extends these results by examining the role of NMDA receptors in the retinogeniculate pathway. First, we studied the normal development of the ferret retinogeniculate projection and found that, after an initial period in which axon arbors extend throughout the height of the LGN, retinal afferents undergo two stages of segregation in achieving the adult form. Axon arbors first become restricted to eye-specific layers and, subsequently, become confined to an inner or outer sublamina within eye-specific layers A and A1. The inner sublamina receives inputs from ON-center cells, and the outer sublamina receives inputs from OFF-center cells (Stryker and Zahs, 1983). These sublaminae are segregated according to differences in cell activity: ON-center and OFF-center retinal ganglion cells have different firing patterns during development (Wong and Oakley, 1996). Furthermore, the process of ON/OFF segregation occurs simultaneously with the maturation of retinal synaptic connections and photoreceptor outer segments (Greiner and Weidman, 1981), suggesting that visually driven activity is important for this patterning. It is known that functional retinogeniculate synapses are present at a very early stage in development (Shatz and Kirkwood, 1984; Campbell and Shatz, 1992; White and Sur, 1992; Mooney et al., 1993; Ramoa and McCormick, 1994; Hohnke and Sur, 1999), indicating that retinogeniculate synaptic transmission occurs prior to retinal afferent segregation. We hypothesized that segregation of ON and OFF inputs would be critically dependent on synaptic transmission between retinogeniculate afferents and LGN cells, particularly on transmission mediated by NMDA receptors. We have addressed this hypothesis by examining the development of the ferret's retinogeniculate projection after a period of blockade of NMDA receptors on LGN neurons—we introduced into the thalamus specific antagonists of NMDA receptors during the period of retinal afferent segregation into ON/OFF sublaminae. A first report of some of these findings was published previously (Hahm et al., 1991).

MATERIALS AND METHODS

Data presented in this study were obtained from 51 neonatal pigmented ferrets (*Mustelidae putorius furo*). Animals were obtained from timed-pregnant jills that were either purchased from Marshall Farms (North Rose, NY) or bred in our colony. The first 24 hours after birth was designated postnatal day 0(P0). The ages studied were P0, P1, P7, P8, P14, P15, P19, P21, P28, and P35. In one set of animals, one eye was injected with anterograde label to visualize laminae and sublaminae. In another set of animals, single axons were labeled by using an in vitro procedure to visualize axon structure. All animal handling and surgical procedures were in accordance with National Institutes of Health guidelines on animal use and followed protocols approved by the Animal Care and Use Committee at the Massachusetts Institute of Technology.

Intraocular injections

Animals were removed from the jill and anesthetized with methoxyflurane (Metofane). In animals in which the eyes were not yet open (P0–P28), the eyelid was swabbed with alcohol, and an incision was made along the future opening. The eye was anesthetized with ophthalmic anesthetic. A hole was punctured in the orbit behind the sclera with a sterile, 26-gauge needle. The tip of a Hamilton syringe (10 µl, 27-gauge needle; Hamilton, Reno, NV) was inserted through the hole into the posterior chamber, and 5–10 µl of a mixed horseradish peroxidase (HRP)/wheat germ agglutinin (WGA) conjugated to HRP (WGA-HRP) solution (20% HRP, 2% WGA-HRP; Sigma, St. Louis, MO) was injected very slowly into the eye. The eyelid was closed and treated with antibiotic ointment. The animal received a subcutaneous injection of amoxicillin (5 mg/kg) and, after recovery from anesthesia, was returned to the mother. After a 24-hour survival, the animal was overdosed with sodium pentobarbital (65 mg/kg) and transcardially perfused with isotonic saline followed by aldehyde fixatives (1% paraformaldehyde and 1.25% glutaraldehyde in 0.1 M phosphate buffer, pH 7.4). The brain was removed and placed in 30% sucrose phosphate buffer overnight (4°C). Subsequently, the brain was embedded in a mixture of albumin and gelatin. Frozen sections were cut at 50 µm in

the horizontal plane, placed in phosphate buffer, and processed for HRP label according to Mesulam (1982) by using tetramethylbenzidine (TMB) as the chromogen. Alternate sections were stained with cresyl violet to visualize cell bodies.

Single axon labeling

The in vitro procedures of Mason (1982) and Sretavan and Shatz (1986) were adapted for ferret tissue. Each animal was deeply anesthetized with sodium pentobarbital (65 mg/kg) and transcardially perfused for 1–2 minutes with cold (4°C), oxygenated (95% O_2, 5% CO_2) artificial cerebrospinal fluid (aCSF), pH 7.4 (1 mM sodium phosphate, 10 mM HEPES, 114 mM NaCl, 5 mM KCl, 2.5 mM $CaCl_2$, 1.15 mM $MgSO_4$, 10 mM dextrose, 25 mM $NaHCO_3$). The animal was placed on a chilled platform, the skull was opened, and the brain was removed quickly and placed in a Petri dish lined with Sylgard and continuously superfused with cold aCSF. The brain was pinned ventral side down through the frontal cortex and cerebellum. The corpus callosum was cut, and each cortical hemisphere was gently lifted up and dissected away from the thalamus by cutting through the internal capsule and cutting away the basal ganglia. The exposed thalamus and midbrain were bisected midsagittally, and each hemithalamus was laid on its medial surface. The pia overlying the LGN was gently peeled away to expose the optic tract.

Glass micropipettes (Frederich Haer, Bowdoinham, ME) pulled to fine tips were dipped in a concentrated solution of HRP and distilled water and allowed to dry, leaving a tiny pellet of HRP adhered to the pipette tip. Under an operating microscope, the pellet was placed manually into the optic tract below the LGN or overlying the ventral LGN. Typically, at least three injections were placed in different regions of the optic tract. After injection, the tissue was placed in a holding chamber containing oxygenated aCSF at room temperature for 3–8 hours to allow the label to transport anterogradely.

After the incubation period, the tissue was immersion fixed overnight in 1% paraformaldehyde and 1.25% glutaraldehyde in 0.1 M phosphate buffer, pH 7.4, and then placed in 30% sucrose phosphate buffer. Prior to sectioning, the two hemispheres were placed with the medial surfaces apposed to each other, held in place with insect pins, and embedded in albumin gelatin. Frozen sections were cut in the horizontal plane at 100 µm then processed for HRP histochemistry by using 3,3′-diaminobenzidine tetrahydrochloride with $CoCl_2$ intensification (Adams, 1981). Serial sections were mounted onto subbed slides, air dried, dehydrated, cleared, and coverslipped.

NMDA receptor blockade

Drug delivery. Animals were implanted with an osmotic minipump (1 µl/hour, 1 week infusion; Alzet model 2001; Alza Corporation, Palo Alto, CA) containing one of the following (in saline) solutions: 1) D-2-amino-5-phosphonovaleric acid (D-APV), 0.8 mM or 0.08 mM (in early experiments, the racemic mixture DL-APV, 1.6 mM or 0.16 mM, was used); 2) L-2-amino-5-phosphonovaleric acid (L-APV), 0.8 mM; 3) (+)-5-methyl-10,11-dihydro-5H-dibenzocyclohepten-5,10-imine maleate (MK-801), 4.75 mM or 1.2 mM; or 4) control vehicle (isotonic saline). D-APV, L-APV, and saline were infused directly into the thalamus, whereas MK-801 and saline were infused subcutaneously.

For intrathalamic infusion, each minipump was connected through a catheter (1.5-cm length of polyvinyl tubing, medical grade) to a 7-mm-long, 28-gauge, stainless-steel cannula (Plastics One, Roanoke, VA). The minipump was implanted subcutaneously, and the cannula was inserted through the cortex and hippocampus and into the thalamus. For subcutaneous infusion, the minipump alone was implanted subcutaneously.

Surgery. All surgical procedures were performed under sterile conditions. At two weeks of age, ferret kits were removed from the mother and prepared for surgery. Animals were anesthetized with ketamine (40 mg/kg body weight) and supplemented with methoxyflurane (Metofane, 1–2%) as necessary. Atropine (0.04 mg/kg) was administered to prevent congestion. For subcutaneous infusion, the skin over the skull was incised and separated from subcutaneous tissue at the back of the neck to create a pocket for the minipump. The minipump was slipped into the pocket, the skin was sutured, and the animal was allowed to recover. For infusion directly into the thalamus, after the skin pocket was created for the minipump, connective tissue was cleared away from the top of the skull with a dry cotton swab. A small hole was drilled in the skull overlying rostral thalamus approximately 2 mm caudal and lateral from the Bregma sutures. The dura was punctured with a 26-gauge needle. After placing the minipump into the skin pocket, the cannula was inserted into the thalamus and glued to the top of the skull with cyanoacrylate glue and then was held in place with dental acrylic. The skin was then sutured, and the animal was allowed to recover and was returned to the mother. The animal received daily injection of a broad-spectrum antibiotic (amoxicillin, 5–10 mg/kg) for 7 days until it was killed.

In placing the cannula within the thalamus, care was taken to avoid positioning the cannula tip too close to the medial border of the LGN. The area targeted for placement of the tip was the anterior thalamus, approximately 2 mm rostral and medial to the LGN and 1 mm below the thalamic surface. At this distance, there was no danger of damaging the geniculocortical fibers in the optic radiations, which may have affected the target cells. Furthermore, this distance is believed to be enough to avoid nonspecific effects of drug release and, according to the dilution curve calculated by Bear et al. (1990), appropriate to deliver a drug concentration adequate to achieve receptor block in these young animals (Esguerra et al., 1992; Ramoa and McCormick, 1994).

Each cannula was tested after perfusion to ensure that drug delivery was free flowing. Animals in which drug delivery was impaired due to blockage of the cannula tip or disconnection of the catheter from the minipump were not considered further. Furthermore, animals in which the cannula was displaced or that received damage to critical areas were not included in the analysis.

For intraocular injections, animals received an injection of WGA-HRP into the eye contralateral to the thalamic implant after 5–6 days of chronic infusion. For consistency, animals that received subcutaneous infusion were injected in the left eye. After a 24-hour survival, animals were perfused, and the brains were removed and processed as described above. For the single axon study, animals received 5–7 days of chronic infusion and then were killed and used in the in vitro procedure described above.

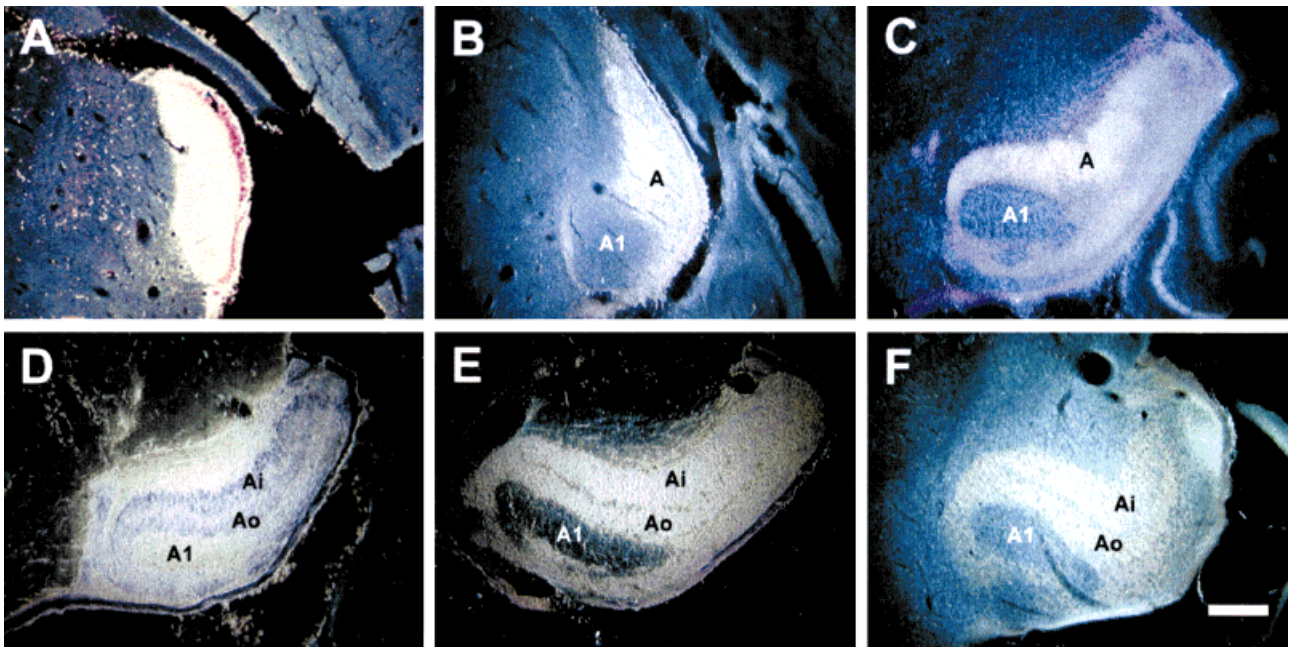

Fig. 1. Photomicrographs of lateral geniculate nucleus (LGN) sections in which the contralateral eye was injected with horseradish peroxidase (HRP)/wheat germ agglutinin (WGA) conjugated to HRP (HRP/WGA-HRP). All sections are in the horizontal plane; anterior is up, and lateral is to the right. **A:** Postnatal day 1 (P1): Retinal afferents are intermixed throughout the extent of the nucleus, and there is little indication of segregation into eye-specific zones. The LGN is a thin band of cells at the anterior thalamus. **B:** P7: First clear indication of afferent segregation according to eye of origin. Laminar borders are undefined, but A and A1 laminae are beginning to form. C laminae have not yet formed. **C:** P15: Afferents are well segregated into eye-specific laminae; the A, A1, and C laminae (posteriorly, adjacent to the optic tract) are clearly established, as are interlaminar zones. **D:** P21: Axons are segregated into ON (Ai) and OFF (Ao) sublaminae within the A layers. Interlaminar and interleaflet zones are distinct, and the LGN begins to take on its adult appearance. **E:** P28: The LGN begins to look more adult-like. ON (Ai) and OFF (Ao) sublaminae are firmly established. **F:** P35: The LGN is essentially adult-like in organization. Scale bar = 250 μm.

Data analysis and axon reconstruction

Serial sections were examined for labeled retinogeniculate axons. Axons were reconstructed with camera lucida on a Leitz Diaplan microscope (Leitz, Wetzlar, Germany) by using ×63 and ×100 objectives under oil immersion with both transmitted light and differential interference contrast microscopy. An Olympus microscope (Olympus, Tokyo, Japan) also was used for some axons with ×50 and ×100 oil-immersion objectives.

To determine the degree of sublamination, a "blind" observer scored the LGN sections by using a scale from 0 to 3, according to the fraction of the A layer that was visibly divided by a staining intensity minimum (Cramer et al., 1996). Horizontal sections through comparable middle portions of the LGN contralateral to eye of injection were examined in each animal. If one in two sections was treated with HRP-TMB, then seven or eight sections were examined. If one in three sections was treated, then five or six sections were examined. The mean sublamination score for all sections scored within an animal was averaged, and each animal was given a single sublamination score.

Photomicrographs of HRP labeling of LGN from eye injections were taken with a ×4 objective by using bright-field or darkfield illumination. Digital images of LGN sections were obtained by using a CCD camera (DKC-5000; Sony Corporation, Tokyo, Japan) mounted onto a Leitz microscope and connected to a computer equipped with a frame grabber running a specialized software (Photoshop, version 3.0; Adobe Systems, Mountain View, CA). By using the same software, the resulting images were then cropped and mounted together to obtain the composite images shown in the figures. Brightness and contrast of the separate portions of each image were matched, and lettering and scale bar were added.

RESULTS

Normal development

Intraocular injections. Injections of HRP/WGA-HRP into the eye resulted in dense label of the optic tract, LGN, and superior colliculus. The position of the ferret LGN changes in the first five weeks of postnatal development (Fig. 1). On the day of birth, it is a relatively flat sheet of cells attached anteriorly in the thalamus; by P35, it has become a garlic clove-shaped structure in the posterior thalamus. During this period, the LGN also rotates such that the anterior portion is displaced laterally, and the posterior segment is displaced medially (Linden et al., 1981; see also Hutchins and Casagrande, 1990). Viewed in horizontal section, the nucleus changes from a thin crescent-shaped wedge of undifferentiated cells to an L-shaped, laminated structure in which the thinner monocular segment runs roughly anterior-posterior longitudinally, and the binocular segment runs mediolaterally.

On P1 (Fig. 1A) retinal afferents from both eyes are intermixed within the LGN. In cases in which the whole eye was injected with HRP, there is no evidence of fibers

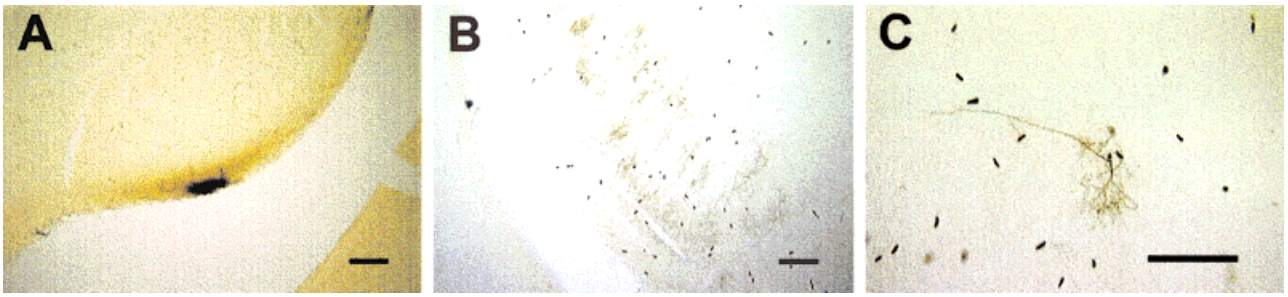

Fig. 2. Photomicrographs depicting site of single-axon HRP injection and type of labeling obtained. **A:** Typical injection site of in vitro axon fills. This is a P35 case; injection is confined to the optic tract. **B:** Labeling obtained with the in vitro axon label method. Axons are well filled and show no signs of degeneration. **C:** Higher power example of axon arbor. Scale bar = 100 μm.

projecting to the perigeniculate nucleus (PGN); however, in cases in which single axons were labeled (see below), bundles of axons are observed that course through the LGN and continue through the PGN. No projection to nonvisual structures, such as the medial geniculate nucleus (MGN) or the inferior colliculus, is seen. By P7, segregation into eye-specific laminae has already begun, and areas of separation are clearly visible. However, afferents are still somewhat intermixed (Fig. 1B), especially in the presumptive A1 lamina. Interlaminar zones are not yet well established, as observed in Nissl-stained material. At this and later ages, streams of fibers can be seen clearly coursing through the PGN; these likely are retinal ganglion cell axons that enter the LGN through the PGN (see also Linden et al., 1981; Roe et al., 1989). By the end of the second postnatal week (P14–P15; Fig. 1C), the A, A1, and C laminae are well defined, and interlaminar zones also are evident in Nissl-stained sections. During the third postnatal week (by P19–P21), the sublaminar leaflets form in the A and A1 laminae (Fig. 1D). In the case shown in Figure 1D, the HRP labeling in the LGN was particularly heavy, causing the reaction product to appear purple under darkfield illumination. Thus, in the photomicrograph shown in Figure 1D, lamina A appears dark, whereas lamina A1 as well as the PGN rostral to lamina A appear bright due to label in fibers of passage. Through the fourth and fifth postnatal weeks (P28–P35), the LGN becomes essentially adult-like in shape, location, and organization (Fig. 1E,F). The eyes open at about P30.

Single axon arbors. The in vitro labeling method resulted in well-filled axons that could be traced reliably back from the LGN into the optic tract. Figure 2 illustrates an example of a typical injection site (Fig. 2A) and the labeling that results from the injection (Fig. 2B,C). Axons were densely labeled with little fading of label at branch points or at the tips of branches. Cut endings or branches were clearly distinguishable from terminal endings. Generally, axon arbor reconstructions spanned a series of three or four sections, although some arbors were contained entirely within one section, and some spanned more than nine sections. For reconstruction, every effort was made to select axons from different levels in the LGN and from all portions of the nucleus, including the monocular segment and binocular projection zones. However, it must be recognized that, of necessity, the axons chosen were the more isolated axons, which were easier to reconstruct. Axons were chosen from the middle sections through the nucleus, avoiding the most dorsal sections, in which laminar boundaries are not distinct, and the most ventral sections, in which the ipsilateral A1 lamina is not present. The major features of arbors in each age group are described below.

P0–P1. At P0–P1, cellular laminae and interlaminar zones are not yet present within the LGN, and retinogeniculate axons are relatively primitive in structure. Most axons have a single main trunk crossing the extent of the nucleus, some ending in a few major forked processes (Fig. 3). However, it is not possible to determine from their morphology whether these processes are the beginning of a terminal arbor or bifurcations in the trunk. Other axons run along the optic tract and send several collaterals into the body of the nucleus.

Axons have occasional side branches along the main trunk that protrude into both presumptive contralateral and ipsilateral zones. In addition to side branches, many axons have extremely fine fibrils studded along their extent. These fibrils appear to be <0.1 μm in diameter and are much thinner than the more obvious side branches, which are similar in thickness to the main trunk. Most of these fibrils are very short (<1 μm) and appear to be hair-like extensions of the axon membrane rather than true axonal branches. Other fibrils, however, extend up to 100 μm from the main trunk and form some fairly elaborate networks (see, e.g., Fig. 3, axons 6 and 7). Side branches do not appear to be restricted to one lamina; indeed, some axons have such branches in both presumptive contralateral and ipsilateral areas (i.e., regions corresponding to the future lamina A and A1). Some axons bifurcate early in their invasion of the LGN and send out widely diverging collaterals that extend in width over one-third of the nucleus (Fig. 3, axon 6). Others bifurcate later and branch in a more limited region of the nucleus (Fig. 3, axons 1, 4, 8, and 9).

At P0–P1, some labeled axons travel in the optic tract and enter the LGN but continue through the nucleus into the PGN. These axons are distinct from the retinogeniculate axons described above in several ways. First, they do not make any side branches or bifurcations within the LGN. Second, these fibers always travel in bundles that remain tightly fasciculated throughout their trajectory. Third, they tend to be thicker and more "kinked" than retinogeniculate axons, as though they were maneuvering around cell bodies. From these characteristics, it is unlikely that these fibers terminate within the LGN. They may belong to a class of nonretinal axons that travel in the optic tract (Reese, 1987), or they may be optic axons projecting to the midbrain. Their ultimate destination is not clear from our material, although some could be seen continuing caudally toward the midbrain. These axons

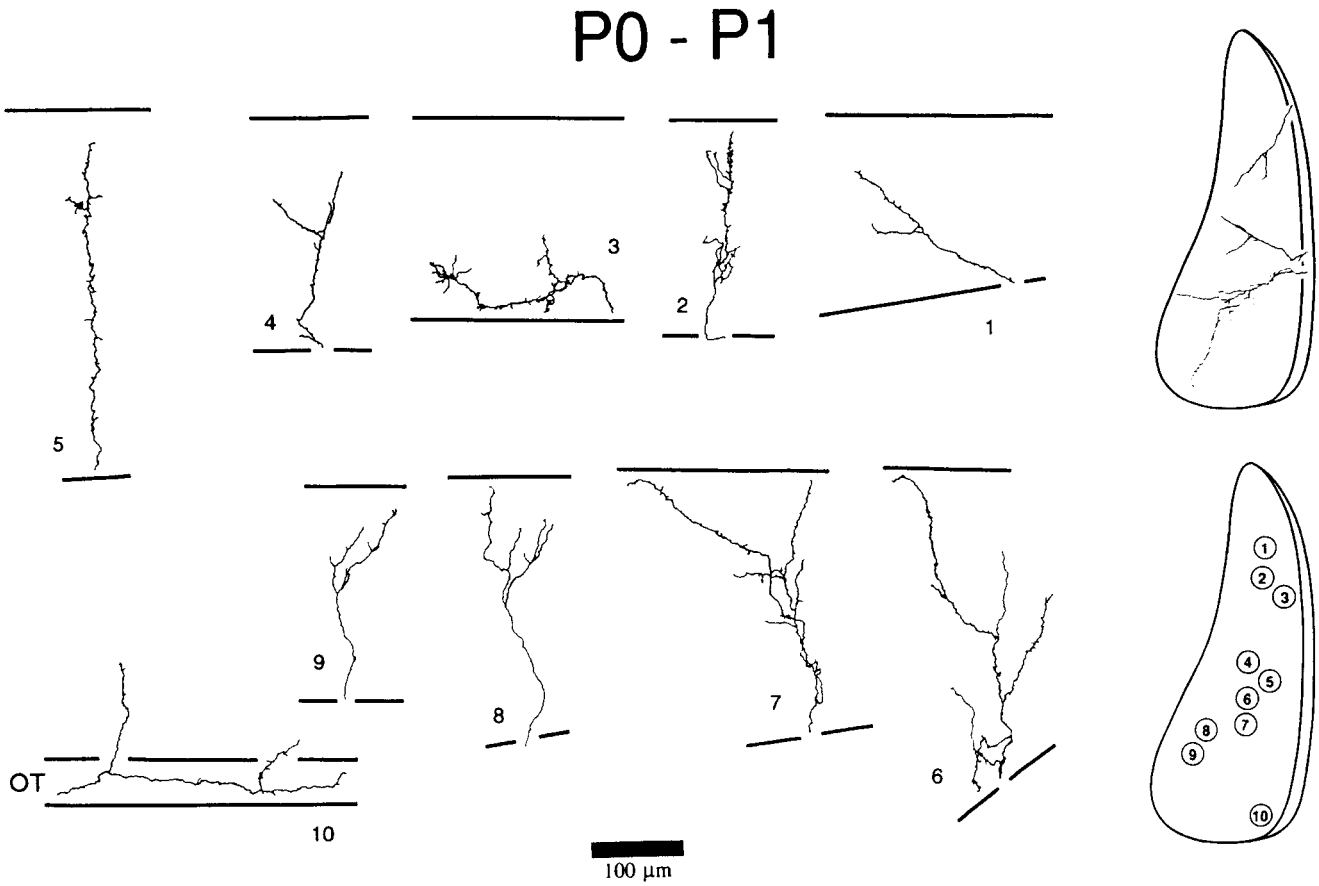

Fig. 3. Camera lucida drawings of axons recovered at P0–P1. In this and all figures that show axon reconstructions, axons are depicted from top right to bottom left according to their location from lateral to medial within the LGN. The optic tract (OT) is at the bottom in all reconstructions. Axons were found in all sections of the nucleus: Only those axons from the middle sections of the nucleus were reconstructed. Axons generally extend to the medial boundary of the nucleus. Many have bifurcating branches and are studded with side branches (for a detailed description, see text). Top right: Location of three representative axons within the LGN. Bottom right: Schematic showing approximate location of each axon within the nucleus. The section depicts a composite of many sections within the LGN.

show no evidence of terminating in the PGN, i.e., there are no branches or defasciculation of bundles. Unfortunately, they could not be followed any farther, because the label did not extend beyond the PGN.

P7–P8. At this age, axons exhibit the first indications of an adult-like arbor (Fig. 4). The main trunks are smooth with occasional minor side branches. The fine, hair-like fibrils are no longer evident. Terminal arbors are fairly rudimentary, and the branch endings are capped with growth cones. Arbors are very widespread: branches extend laterally in all directions from the arbor and have not yet coalesced into the dense plexus of branches that characterizes arbors at later ages.

The most notable characteristic of these arbors is that they are spread across a region approximately one-third to half of the thickness of the nucleus (this dimension, the distance perpendicular to laminar borders, is referred to hereinafter as the "height" of the nucleus). Although definitive laminar boundaries were not visible in our material at this age (however, see Hutchins and Casagrande, 1990), the HRP label from eye injections (Fig. 1B–E) indicates that such a distance corresponds to one eye-specific layer. It must be emphasized, however, that arbors are not totally restricted to a presumptive eye-specific layer. Arbors still have branches that extend across presumptive laminar boundaries.

P14–P15. At this age, cellular laminae and interlaminar zones are evident. Axon terminal arbors are more dense and more elaborate in the pattern and complexity of their branching (Fig. 5). Overall, the arbor appears to become more compact. Widespread branches are infrequent, although some axons still have a few branches projecting away from the core of the arbor. Arbors also appear somewhat shorter in height than at earlier ages, presumably because the terminal arbor has become more confined to one eye-specific layer. Thus, any stray side branches near laminar boundaries most likely have been eliminated. In our eye injection material, sublaminar leaflets are not evident at this age (Fig. 1C), and this also is reflected in the individual retinogeniculate arbors. Terminal arbors extend across most of the eye-specific lamina, but most arbors do not appear to reach from one laminar boundary to the other. In one instance, as a possible indication of sublaminar segregation about to occur, one of the axons (reconstructed in Fig. 5, axon 2) was confined completely to the outer portion of lamina A.

P19–P21. At this age, sublaminar leaflets have formed, although interleaflet zones are not yet clearly established.

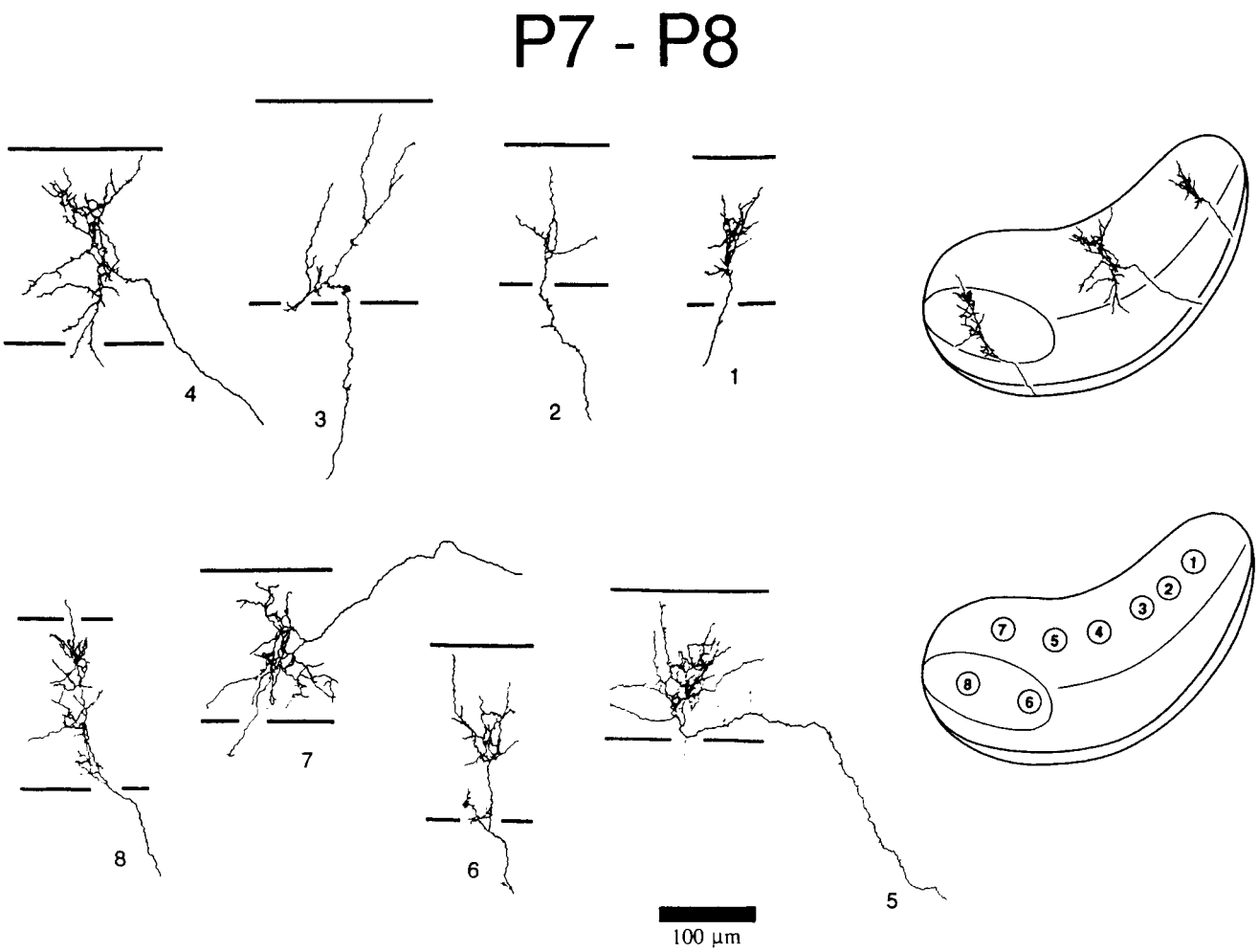

Fig. 4. Camera lucida drawings of axons reconstructed from P7–P8 cases. Axons are depicted lateral to medial (for conventions, see Fig. 3 legend). The first indication of terminal arbors is seen at this age, although side branches still are present. Top right: Schematic showing location of representative axons in the nucleus. Laminar borders, although they are not yet clear, are drawn according to eye injection data for clarity. Axons are not to scale. Bottom right: Drawing of LGN indicating the position of each axon within the nucleus. Axon 4 after Smetters et al. (1994; see Fig. 5).

Examples of retinal axons are illustrated in Figure 6A,B. Axon trunks appear to be somewhat thicker than at earlier time points, and arbors clearly are restricted to one sublaminar leaflet. The arbor framework is long and narrow, with the longitudinal axis perpendicular to laminar borders. The arbor core is much more dense at than previous ages and more confined to its target zone. There is relatively little encroachment over putative sublaminar boundaries: One or two branches may extend a short distance into another sublaminar leaflet. Most arbors have branches that extend to the edges of the sublamina.

P28–P35. Axon arbors essentially are adult-like at this age. The arbor is a narrow, dense plexus of branches that is confined tightly to its target zone (Fig. 7). P28 is the first age examined at which terminal bouton clusters are visible on branches. They are present simultaneously with growth cones on the same arbor. By P35, growth cones have disappeared and largely have been replaced by terminal boutons.

Quantitative measures of arbors. To quantify the changes in arbor development during the first five postnatal weeks, measurements were taken of the height, width, and area of each axon arbor. For all ages, we defined the beginning of the arbor at the first major branch point in the axon trunk within the LGN, a major branch being defined as at least 20 µm long. The height of an arbor was determined as the extent of the arbor orthogonal to laminar borders, from the first branch point to the most distal arbor tip. Arbor width was defined as the extent of the arbor parallel to laminar border, encompassing the outermost branch tips. Arbor area was computed as the area within an outline encompassing the outermost branch tips around the arbor. Means were obtained by measuring arbors at each age and pooling the values across animals (Table 1).

We computed the arbor height in relation to the height of the LGN where the arbor was located to get an accurate portrayal of how arbor size may relate to target size. To achieve this, a line was drawn along the arbor height axis until it intersected the LGN boundaries (most often, approximately perpendicular to the boundaries), and the distance between LGN borders was defined as the LGN

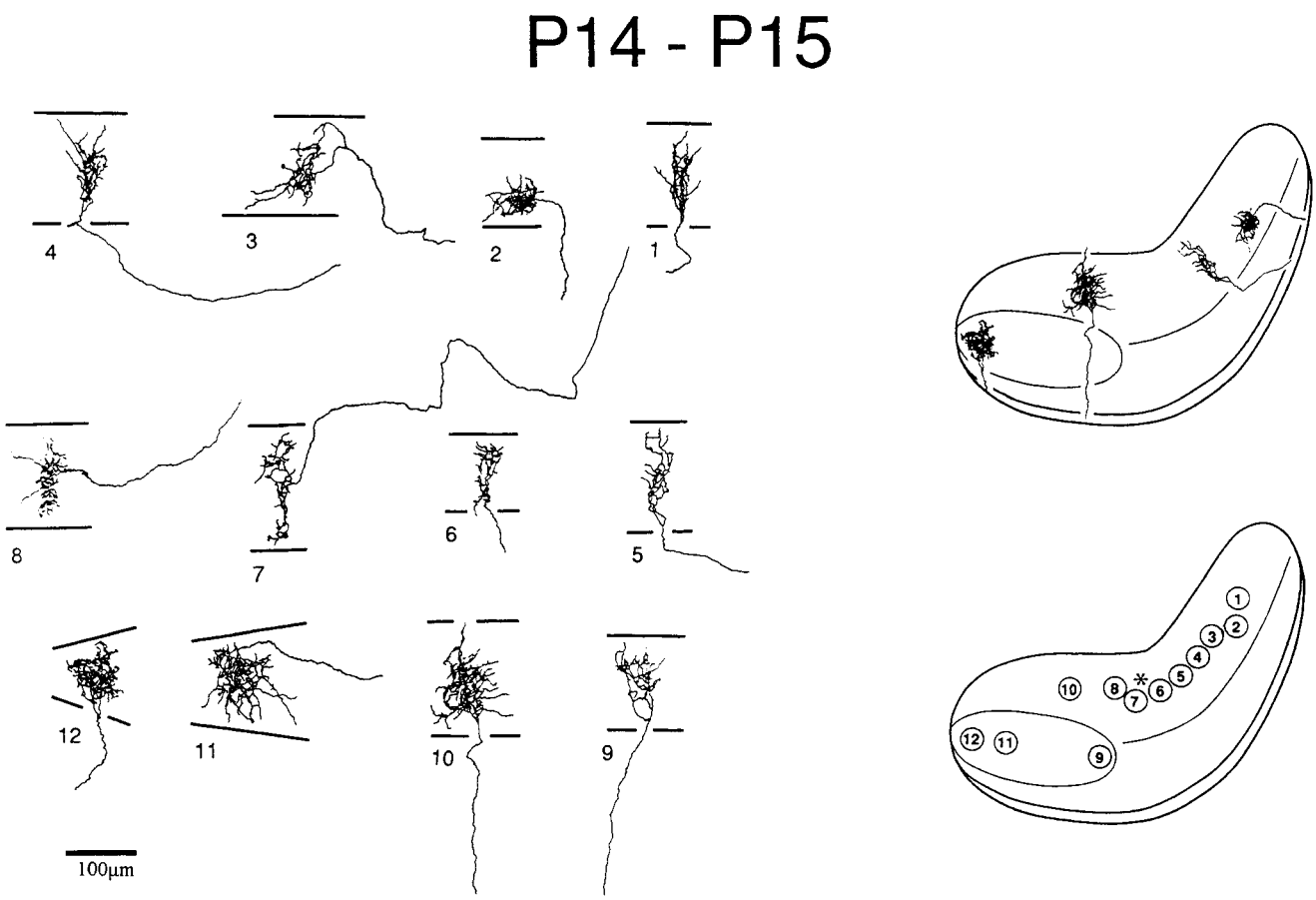

Fig. 5. Camera lucida drawings of axons from P14–P15 cases. Axons have denser terminal arbors that appear more restricted to an eye-specific layer. Side branches have disappeared. Top right: Schematic drawing of LGN depicting representative axon arbor locations. The laminar boundaries are very distinct at this age (see Fig. 1C). Axons are not to scale. Bottom right: Schematic showing location of each axon within the LGN. Asterisk marks an axon in which the arbor could not be reconstructed fully. Axons 1 and 3 after Hahm et al. (1991; see Fig. 2).

height for that particular axon. LGN heights varied considerably within a single section, because axons were reconstructed from the thin monocular segment as well as the thicker binocular segment. LGN width was measured from the most anterior and lateral LGN boundary to the most medial and caudal LGN boundary, along a line bisecting the nucleus parallel to LGN borders. Our measurements reflect LGN dimensions at locations where arbors were found rather than a systematic sampling of LGN size at each age; therefore, the values of LGN height and width obtained do not necessarily reflect average height and width of the LGN at the ages chosen.

Arbor height. The mean height of arbors at each age is depicted in Figure 8A. Arbor height stayed relatively constant from P0–P1 to P7–P8 but decreased by P14–P15. This decrease was significant (P7–P8 vs. P14–P15; $P < 0.05$; Mann-Whitney U test). In the third postnatal week, by P19–P21, there was a significant increase in arbor height (P14–P15 vs. P19–P21; $P < 0.05$). At P28–35, arbor height was slightly smaller, but not significantly so (P19–P21 vs. P28–P35; $P = 0.16$).

The ratio of arbor height to LGN height (Fig. 8B) tended to decrease from P0–P1 to P28–35. When axon measurements were averaged to obtain a single datum from each animal, a linear regression yielded a significant relationship ($R = 0.81$; $P < 0.005$). At ages when true arbors are present and laminar borders evident (P14 and older), arbor heights also were assessed in relation to eye-specific lamina height. Lamina heights were measured in the same manner as LGN heights. Figure 8C shows that the ratio of arbor height to lamina height similarly decreased significantly with age ($R = 0.86$; $P < 0.005$).

Arbor width. Arbor width (Fig. 9A, Table 1) was relatively constant, varying from 118 μm at P0–P1 to 78 μm at P28–P35. None of the differences in size at any of the ages was significant, and a linear regression analysis showed no significant change in arbor width with age ($R = 0.166$; $P > 0.1$). A comparison of arbor width relative to LGN width is shown in Figure 9B. The decrease in arbor width/LGN width with age was not significant ($R = 0.119$; $P > 0.1$).

Fig. 6. **A,B:** Camera lucida drawings of axons from P19–P21 cases. Left: Axon arbors are now confined to sublaminar leaflets and are branched more densely. Top right: Schematic drawing of LGN depicting representative axon arbor locations. Axons are not to scale. Bottom right: Schematic showing location of each axon within the LGN. Asterisks mark axons in which the arbors could not be reconstructed fully. Axons 1 and 2 after Hahm et al. (1991; see Fig. 2).

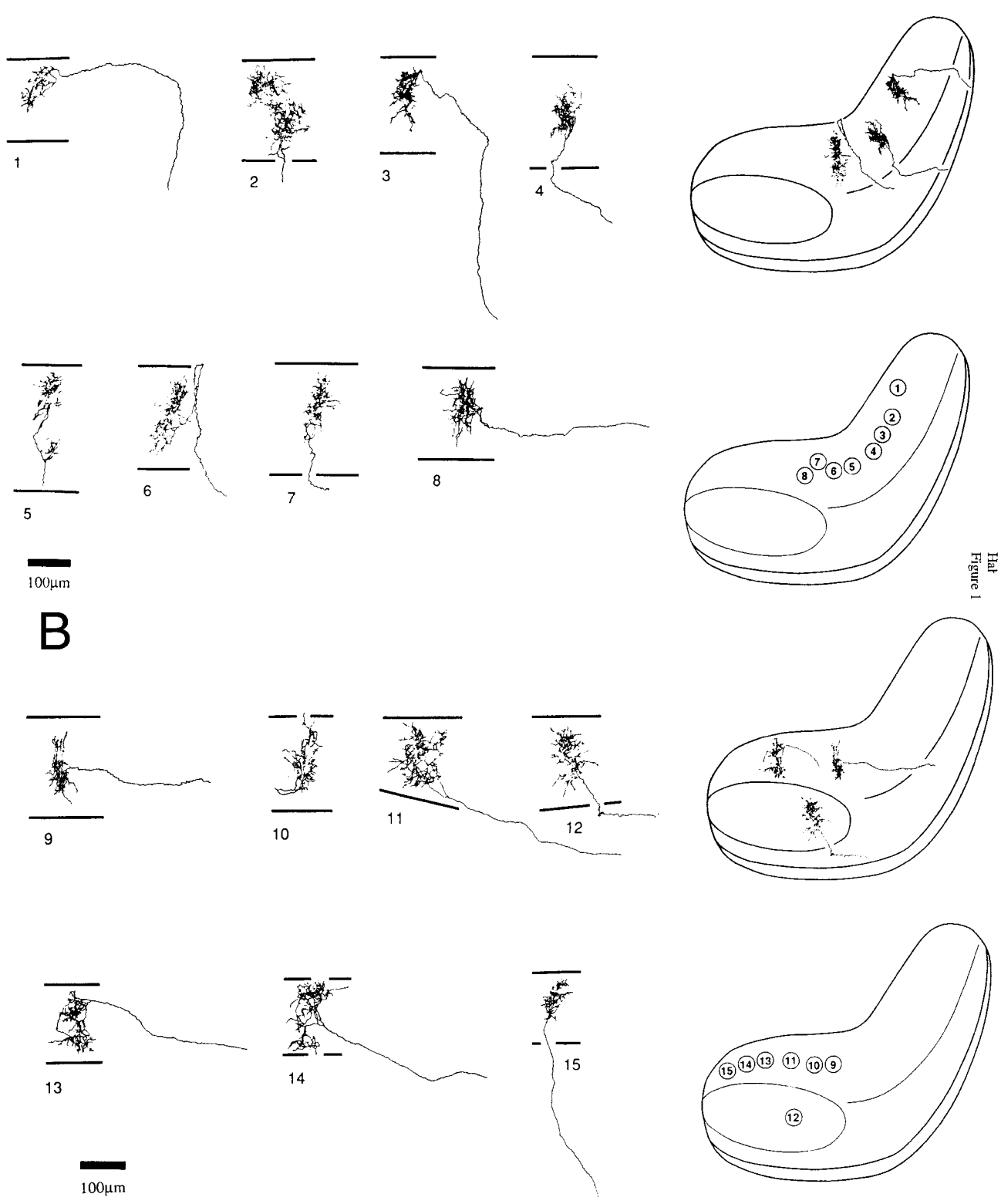

Figure 6

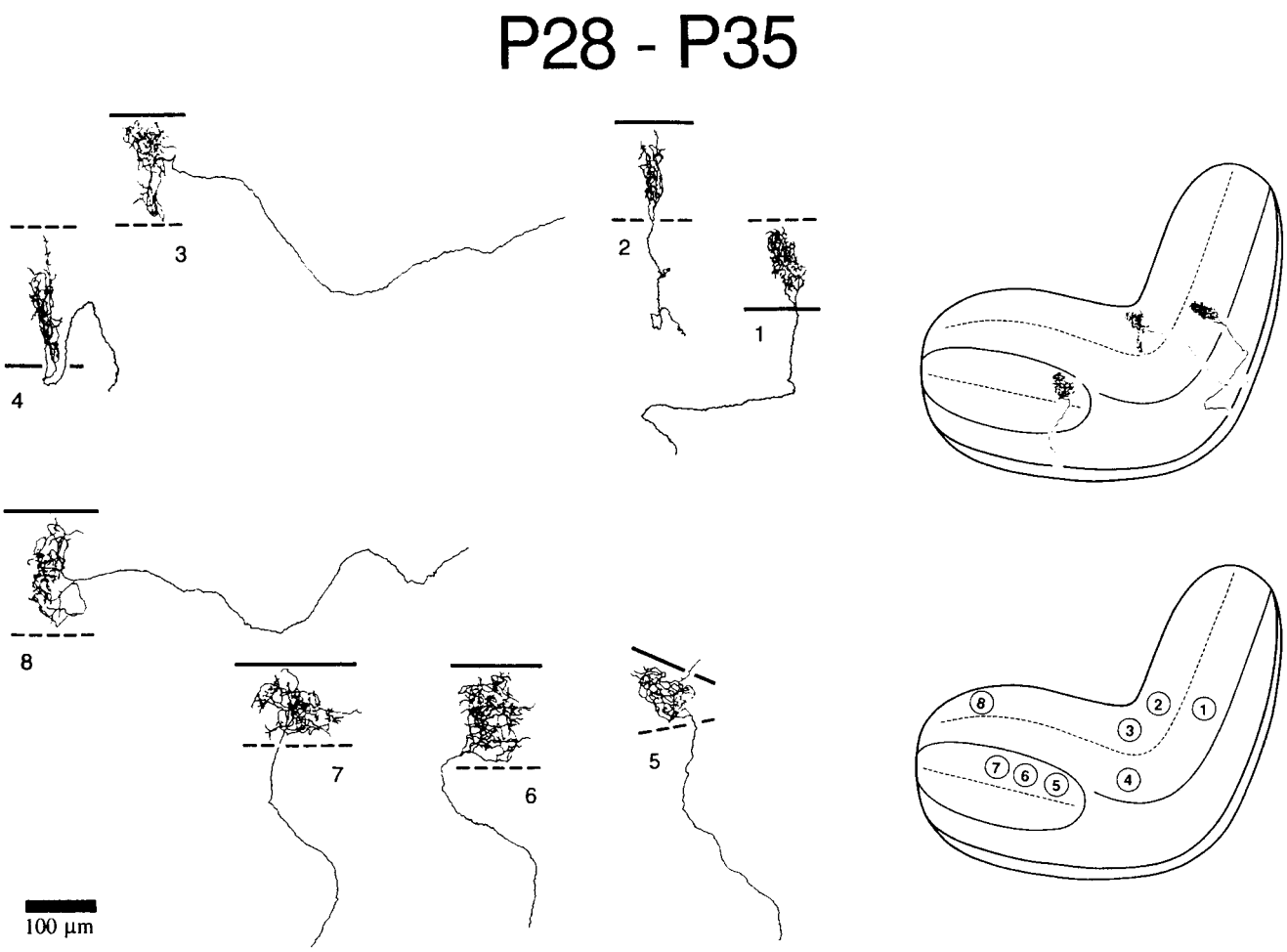

Fig. 7. Camera lucida drawings of axons from P28–P35 cases. Arbors are essentially adult-like, and terminal boutons are visible on many arbors. Top right: Schematic drawing of LGN depicting representative axon arbor locations. Axons are not to scale. Bottom right: Schematic showing location of each axon within the LGN.

TABLE 1. Development of Retinogeniculate Axon Arbors

Age[1]	Number of animals, eye injections	Number of animals, single axon analysis	Number of axons reconstructed	Arbor height, µm (mean ± S.E.M.)	Arbor width, µm (mean ± S.E.M.)	Arbor area, µm² (mean ± S.E.M.)
P0–P1	6	3	10	177.4 ± 23.8	118.3 ± 29.3	—
P7–P8	4	2	8	165.3 ± 17.7	94.6 ± 14.1	6,491 ± 1,161
P14–P15	3	3	13	123.7 ± 9.3	77.9 ± 6.35	5,138 ± 602
P19–P21	3	3	17	158.2 ± 7.9	90.2 ± 7.7	7,718 ± 686
P28–P35	2	3	8	139.9 ± 12.1	78.3 ± 11.5	6,450 ± 837

[1]P, postnatal day.

Arbor area. The area of LGN covered by axon arbors is shown in Figure 9C. Arbor areas were measured from the onset of arborization (P7–P8) to the oldest ages examined (P28–P35). Arbor areas showed a slight but nonsignificant reduction from P7–P8 to P14–P15 ($P = 0.25$). From P14–P15 to P19–P21, arbor areas increased significantly ($P < 0.01$) and remained relatively unchanged at P28–P35 (P19–21 vs. P28–35; $P = 0.24$). The fact that sublaminar segregation during the third postnatal week is accompanied by an increase in absolute arbor area suggests that the growth of the LGN itself is proportionately greater than the increase in arbor area and, hence, is a key determinant of afferent patterning.

NMDA receptor blockade

Intraocular injections. Figure 10 shows darkfield photomicrographs of the right LGN of animals that received an injection of HRP into the left eye. The LGN of a normal P21 animal is depicted in Figure 10A, illustrating that retinal afferents have segregated into inner (ON) and outer (OFF) sublaminae in the contralateral lamina A. The degree of segregation was evaluated by using a sublamination score (see Materials and Methods). The sublamination scores of animals in all conditions examined in this study are shown in Table 2 and Figure 11. The sublamination score was significantly greater in normal P21 animals

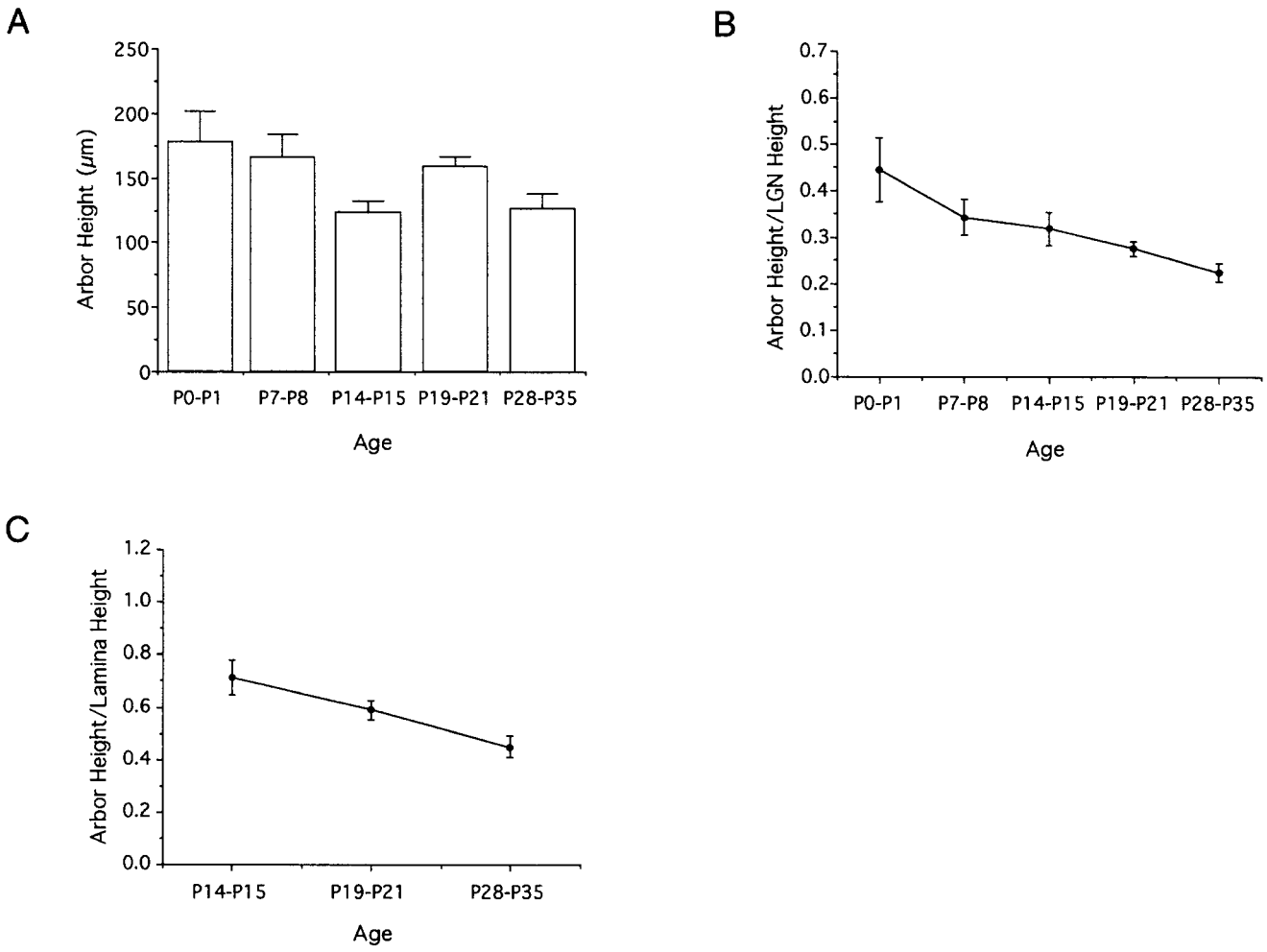

Fig. 8. Graphs of axon arbor height. **A:** Heights of axon arbors plotted as a function of age. **B:** Arbor heights as a ratio of LGN height plotted as a function of age. **C:** Arbor heights as a ratio of eye-specific lamina height plotted as a function of age.

than in normal P14 animals (see Fig. 1C, D; $P < 0.05$; Mann-Whitney U-test). Figure 10B shows the LGN of a control animal that received intrathalamic infusion of saline from two weeks of age to three weeks of age. The retinal afferents were segregated into sublaminar leaflets: The sublamination score for saline-treated animals (Fig. 11) was not different from normal P21 animals ($p > 0.2$). Treatment with L-APV had a similar effect.

Treatment with D-APV and MK-801 during the third postnatal week disrupted sublamination and produced a decrease in sublamination scores. We used D-APV (Fig. 10C,D) at doses of 0.8 mM and 0.08 mM. The sublamination score (Fig. 11) for animals treated with 0.08 mM D-APV was higher than that for animals treated with 0.8 mM D-APV; a linear regression analysis of D-APV dose and sublamination score showed a significant change ($R = 0.87$; $P < 0.05$). MK-801 was used at doses of 4.75 mM and 1.2 mM (Fig. 10E,F). The sublamination score (Fig. 11) decreased at a high dose of MK-801 ($R = 0.82$; $P < 0.01$). Thus, high doses of NMDA antagonists prevent sublaminar segregation, whereas low doses do not.

Single axon morphology.

Qualitative differences. Retinogeniculate axon arbors in animals treated with 0.8 mM D-APV are illustrated in Figure 12. In general, the overall morphologic structure of D-APV-treated axons is not greatly altered from that of normal axons. Like normal P21 axons (Fig. 6) and drug-control axons (Fig. 13, which shows axons in animals treated with L-APV and 0.08 mM D-APV), each retinogeniculate axon enters the LGN without giving rise to branching collaterals within either the LGN or the optic tract. The axon trunks within the LGN are smooth, with no side branches along their length. Each axon has a single terminal arbor confined to either lamina A or A1.

However, in several ways, axons in D-APV-treated animals differ from those in normal three-week animals (Fig. 6) or axons in control animals (Fig. 13), which have arbors that are confined to an inner or outer sublamina within the A layers. First, some axons have terminal arbors that show no evidence of restriction into a sublaminar leaflet (see, e.g., Fig. 12, axons 2, 5, 6, 11, 13, and 14). These axons span the height of an entire eye-specific lamina, with no biasing of the arbor toward an inner or outer half. Other axons

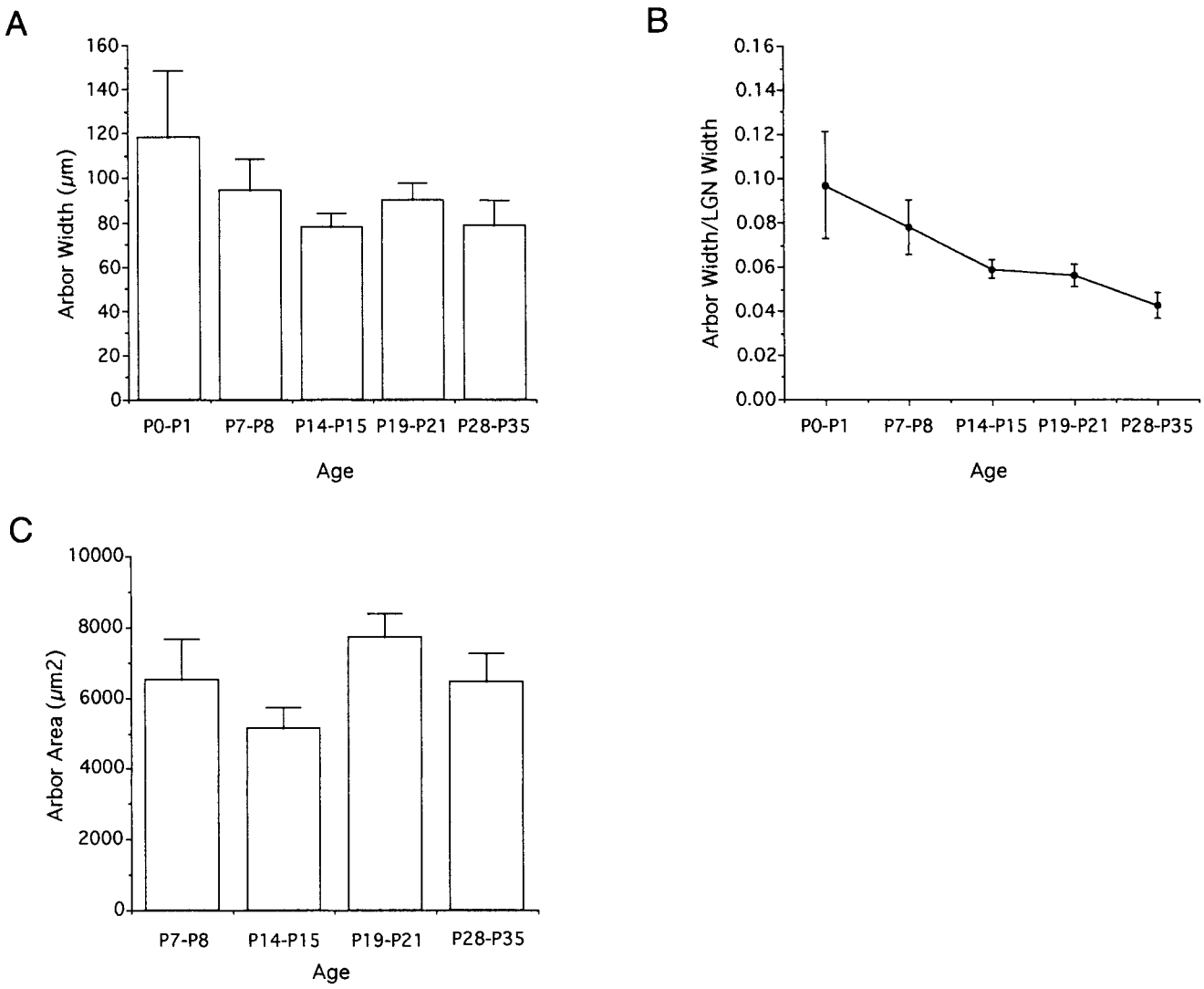

Fig. 9. Graphs of axon arbor width and area. **A:** Widths of axon arbors plotted as a function of age. **B:** Arbor widths expressed as a ratio of LGN width plotted as a function of age. **C:** Arbor area plotted against age.

(see, e.g., Fig. 12, axons 4, 7, 8, 9, and 12) are restricted appropriately in size, such that they would fit into a sublamina, but they are positioned inappropriately toward the center rather than in an inner or outer half of an eye-specific lamina. Still others appear to be restricted appropriately in size and location, being located close to inner or outer laminar boundaries (see, e.g., Fig. 12, axons 1, 3, and 15). Thus, although the morphology of these axon arbors is not changed greatly, the location of arbors is changed in the 0.8 mM D-APV-treated animals compared to both normal and drug-control three-week axons. The unrestricted axons of high-dose D-APV-treated animals are more like those of normal P14 animals, in which axon arbors are confined to an eye-specific lamina but not to a sublamina (Fig. 5).

Quantitative differences. We compared two characteristics of normal and D-APV-treated axon arbors: terminal arbor area and degree of segregation (Table 2, Fig. 14). The axon data from each animal was pooled, and conditions were compared by treating each animal as a single datum.

The arbor areas of normal P14 and P21 animals, 0.8 mM D-APV-treated animals, and drug-control animals are depicted in Figure 14A. Between two and three weeks of age, as discussed above, there is a significant increase in axon arbor size. The mean axon arbor area in normal P21 animals was not significantly different from that in D-APV-treated animals ($P = 0.29$, Mann-Whitney U test) or drug-control animals ($P = 0.56$). Similarly, axons in D-APV treated animals were not different from axons in drug-control animals ($P = 0.16$). However, axons in D-APV treated animals were significantly larger than those in normal P14 animals ($P < 0.05$).

To assess the degree of segregation of each axon, we used a "sublamina index," which measured the greatest proportion of an arbor lying in the inner or outer half of lamina A or A1 (Hahm et al., 1991; Cramer et al., 1996). To accomplish this, we bisected the lamina longitudinally and measured the extent of the arbor on each side of this imaginary line. The larger portion was computed as a

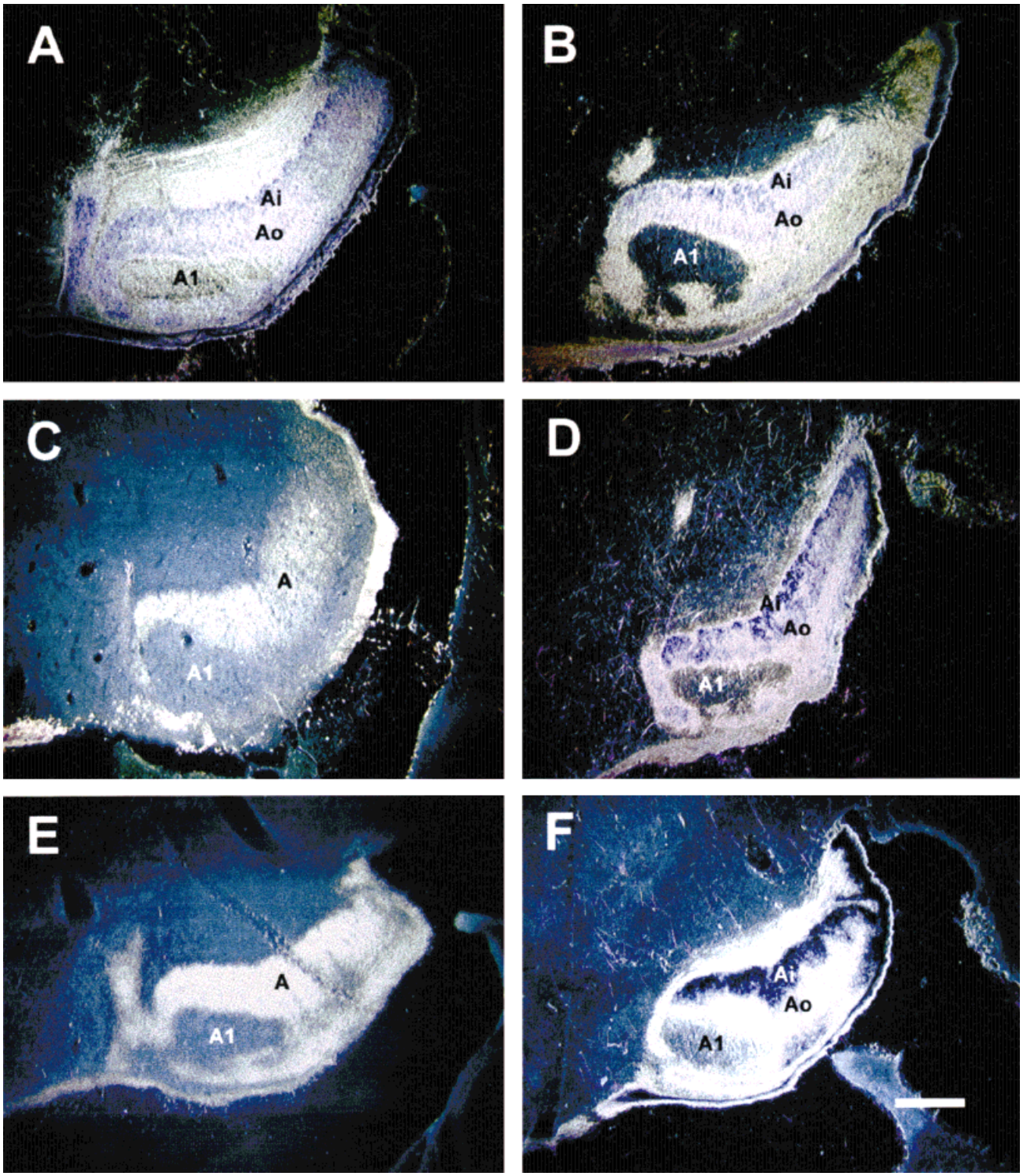

Fig. 10. Darkfield photomicrographs of the right LGN in animals that received an injection of HRP into the left eye. All drugs were infused chronically between two weeks and three weeks of age. **A:** LGN of normal 3-week-old animal. Retinal afferents are segregated into inner (ON; Ai) and outer (OFF; Ao) sublaminae within lamina A. **B:** LGN of a three-week-old animal that received saline infusion. Sublaminae are present within lamina A. **C:** LGN of a three-week-old animal that was treated chronically with 0.8 mM D-2-amino-5-phosphonovaleric acid (D-APV). Retinal afferents are not segregated into inner and outer sublaminae. **D:** LGN of a three-week-old animal that was treated chronically with 0.08 mM D-APV. Retinal afferents are segregated into inner and outer sublaminae. **E:** LGN of a three-week-old animal that was treated systemically with 4.75 mM (+)-5-methyl-10,11-dihydro-5H-dibenzocyclohepten-5,10-imine maleate (MK-801). Retinal afferents failed to segregate into inner and outer sublaminae. **F:** LGN of a three-week-old animal that was treated systemically with 1.2 mM MK-801. Retinal afferents are segregated into sublaminae (sublamina Ai appears blue/purple under darkfield illumination due to differentially heavy transport of label by ON-center axons). Scale bar = 250 μm.

TABLE 2. Effect of N-Methyl-D-Aspartate Receptor Blockade on Sublamina Formation and Axon Morphology

Condition[1]	Number of animals, eye-injections	Sublamina score (mean ± S.E.M.)	Number of animals, single axon analysis	Number of axons reconstructed	Sublamina index (mean ± S.E.M.)	Arbor area, μm² (mean ± S.E.M.)
Two-week normal	3	0.07 ± .03	3	13	0.70 ± 0.03	5,138 ± 602
Three-week normal	3	1.8 ± .35	3	17	0.89 ± 0.06	7,718 ± 686
High-dose APV	2	0.6 ± .6	4	15	0.64 ± 0.03	9,050 ± 1,014
Low-dose APV	1	2.0	1	4	0.81 ± 0.05	7,619 ± 774
L-APV control	2	1.1 ± .5	1	4	0.85 ± 0.08	5,817 ± 67
Saline control	3	2.5 ± .3	—	—	—	—
High-dose MK-801	3	0.5 ± .25	—	—	—	—
Low-dose MK-801	3	1.7 ± .55	—	—	—	—

[1]APV, D-2-amino-5-phosphonovaleric acid; L-APV, L-2-amino-5-phosphonovaleric acid; MK-801, 5-methyl-10,11-dihydro-5H-dibenzocyclahepten-5,10-imine maleate.

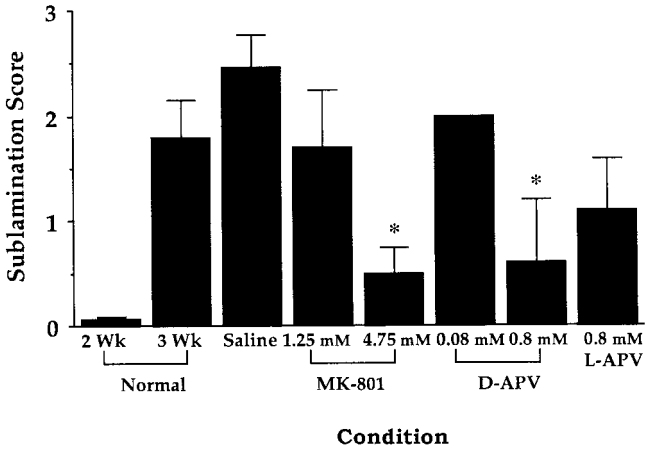

Fig. 11. Histogram summarizing sublamination scores for all of the experimental and control conditions in the study. The sublamination scores, ranging from 0 to 3, were assigned by a "blind" observer and reflect the extent of the labeled A layer that is subdivided by a staining intensity minimum. Scored sections were averaged to obtain a single score per animal. A sublamination score of 3 signifies complete sublamination. Error bars denote S.E.M. Doses of N-methyl-D-aspartate (NMDA) receptor blockers and control drugs are indicated. Higher doses of NMDA receptor antagonists produce greater disruption of sublamination; high doses of MK-801 and D-APV lead to sublamination scores that are significantly lower than low-dose animals, three-week normal animals, or saline control animals (asterisks). L-APV, L-2-amino-5-phosphonovaleric acid.

proportion of the entire arbor area, resulting in a ratio between 0.5 and 1.0. Thus, a sublamina index of 1.0 represents an arbor that is confined entirely to an inner or outer half of lamina A or A1. A sublamina index of 0.5 represents an arbor that is divided equally between the inner and outer halves of the lamina, with no evidence of sublaminar segregation.

The sublamina indices of normal two- and three-week-old animals, D-APV-treated 3-week animals, and drug-control three-week-old animals are shown in Figure 14B. Again, axons were averaged for each animal, and data were compared by treating each animal as a single datum. Between two weeks and three weeks of age in normal animals, the sublamina index increased significantly ($P < 0.05$, Mann-Whitney U test). D-APV-treated axons had a sublamina index similar to that of two-week normal animals ($P = 0.28$) but significantly smaller than that of normal three-week-old animals ($P < 0.05$) or drug-control animals ($P < 0.1$). Hence, treatment with D-APV leads to retinogeniculate axon arbors that are less restricted to one half of an eye-specific lamina than arbors in normal or control animals.

DISCUSSION

In this study, we have described the development of retinogeniculate axons in ferrets from birth to 5 weeks of age and the effect of blocking NMDA receptors in the LGN during the third postnatal week. Retinogeniculate afferents in the binocular segment of the LGN undergo progressive remodeling from an early stage, in which axons from the two eyes are intermixed and project diffusely throughout the LGN, to an adult-like, segregated projection, in which retinal axons form terminal arbors within LGN areas appropriate for the eye of origin and ganglion cell type (ON or OFF). This sculpting of the retinogeniculate projection occurs by directed terminal arbor growth into appropriate LGN layers and sublayers, coincident with the elimination of extraneous branches in inappropriate areas.

Blockade of NMDA receptors during the third postnatal week, when retinogeniculate afferents within eye-specific laminae segregate into ON/OFF sublaminae, prevents this sublaminar segregation. The disruption of the sublaminar pattern results from abnormal arborization of retinogeniculate axons. Individual axons have arbors that are not different in size compared with normal, age-matched arbors but that are positioned inappropriately within each eye-specific lamina. Thus, NMDA receptors on LGN cells significantly influence pattern formation by retinal afferents within the LGN.

Role of NMDA receptors in retinogeniculate patterning

There is considerable evidence now for a role for afferent and target activity in shaping projection patterns in the visual system, including the retinogeniculate pathway. Retinal ganglion cells in mammals are spontaneously active at very early developmental stages (Galli and Maffei, 1988), and neighboring ganglion cells are correlated with one another in their firing (Arnett, 1978; Arnett and Spraker, 1981; Meister et al., 1991; Wong et al., 1993; Wong and Oakley, 1996). Differences in activity between the two eyes and between ON-center and OFF-center retinal ganglion cells from the same eye could serve as a means of differentiating inputs. Blockade of activity with intrathalamic infusion of TTX in fetal cats prevents retinal afferents from sorting into eye-specific laminae (Shatz and Stryker, 1988) and results in grossly abnormal, nonspecific terminal arbors (Sretavan et al., 1988): Blockade of retinal waves with intraocular administration of cholinergic antagonists also prevents eye-specific segregation (Penn et al., 1998). In ferrets, intraocular blockade of afferent action potentials with TTX during the third and fourth postnatal weeks disrupts the formation of ON/OFF sublaminae (Cramer and Sur, 1997). Thus, afferent activity is

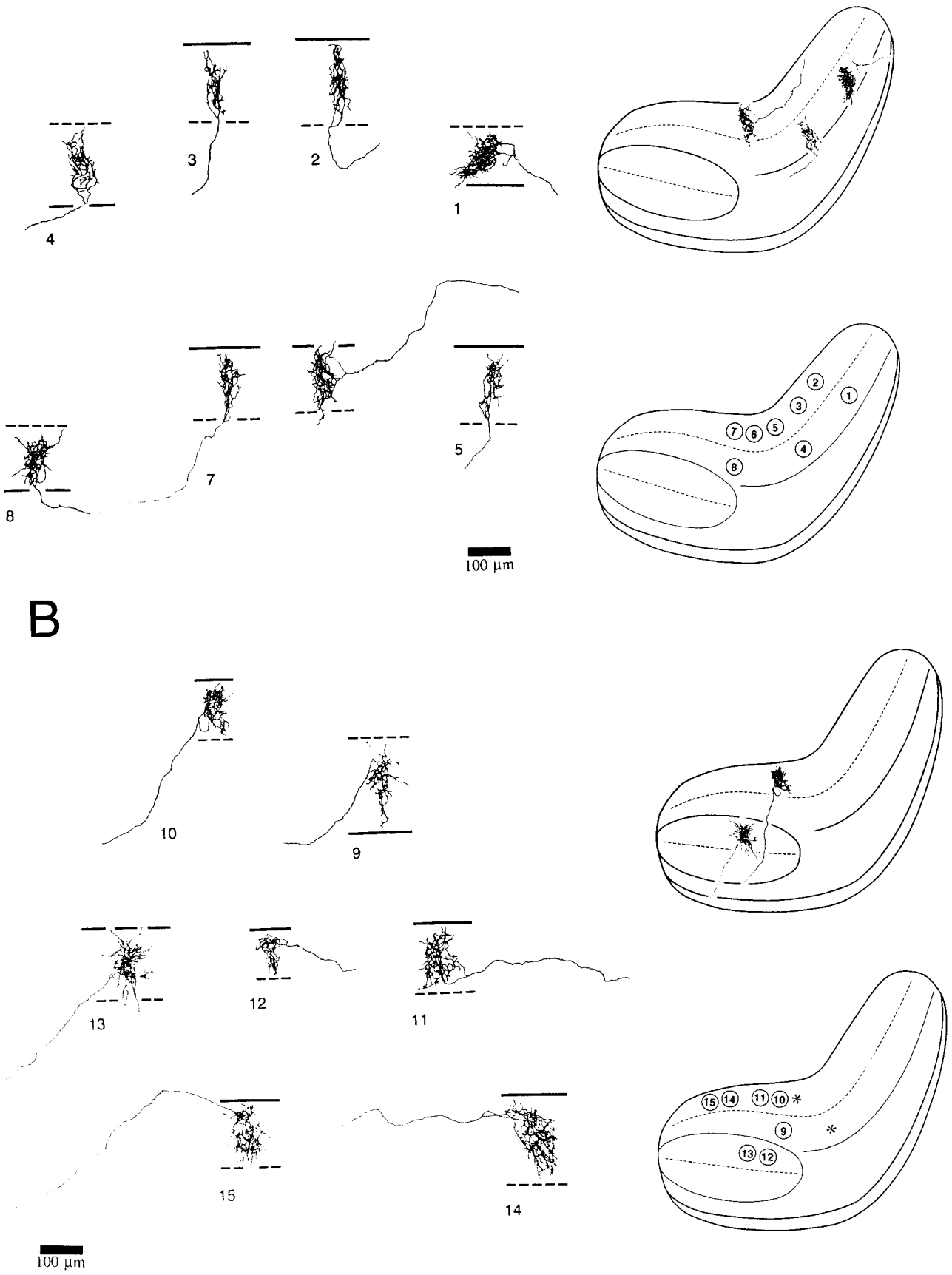

Fig. 12. **A,B:** Reconstruction of retinogeniculate axons recovered from 3-week-old animals that were treated chronically with 0.8 mM D-APV. Top right: Schematic drawing of LGN depicting representative axon arbor locations. Axons are not to scale. Bottom right: Schematic showing location of each axon within the LGN. Axons 4, 9, 14, and 15 after Hahm et al. (1991; see Fig. 2).

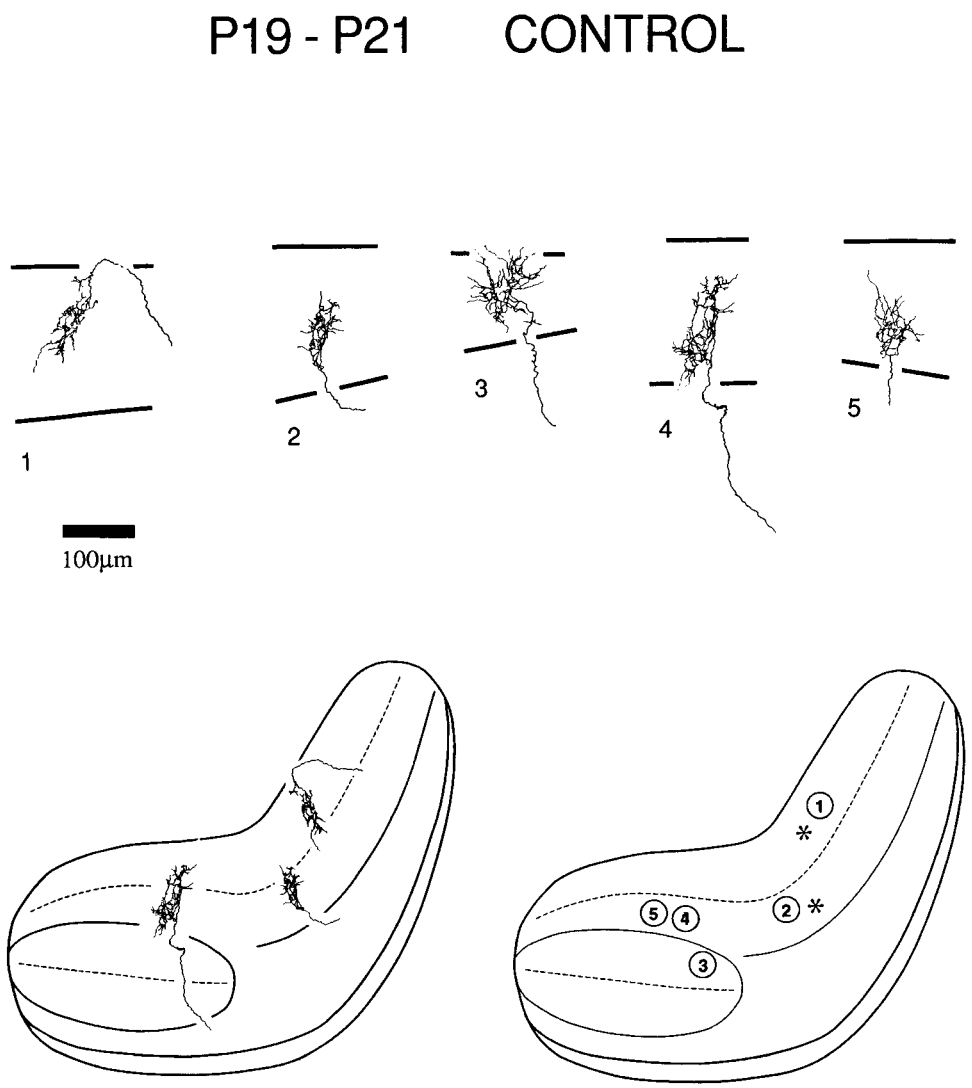

Fig. 13. Reconstruction of retinogeniculate axons recovered from P21 animals that served as drug controls (0.8 mM L-APV or 0.08 mM D-APV). Top right: Schematic drawing of LGN depicting representative axon arbor locations. Axons are not to scale. Bottom right: Schematic showing location of each axon within the LGN. Asterisks indicate arbor locations of axons that could not be reconstructed fully.

important for guiding axon arbor growth at multiple phases of retinogeniculate development.

NMDA receptors can function as correlation detectors and serve to transduce electrical activity into cellular signals that mediate patterns of termination and contact. The effects of NMDA receptor blockade have been examined in the visual cortex of cats (Bear et al., 1990), in which it prevents the ocular dominance plasticity associated with monocular lid suture, and in the retinotectal projection of amphibians, in which it disrupts eye-specific segregation associated with a supernumerary eye (Cline et al., 1987; Cline and Constantine-Paton, 1990) or retinotectal projections associated with map formation (Cline and Constantine-Paton, 1989).

Retinogeniculate synaptic transmission is mediated by NMDA and non-NMDA (α-amino-3-hydroxy-5-methyl-4-isoxazole-propionate; AMPA) receptors in both adult (Hartveit and Heggelund, 1990; Heggelund and Hartveit, 1990; Sillito et al., 1990a,b; Kwon et al., 1991) and developing (Esguerra et al., 1992; Mooney et al., 1993; Ramoa and McCormick, 1994) cats and ferrets. Thus, NMDA receptor blockade reduces retinogeniculate transmission and the activity of target cells in the LGN. One possibility to be kept in mind when considering our results (and others mentioned above) is that they derive from a generalized reduction in activity of LGN (or other target) cells rather than from a specific blockade of NMDA receptors. Furthermore, NMDA receptor blockers may act nonselectively on other receptor types on developing neurons or may reduce or suppress the expression of AMPA/kainate receptors (Constantine-Paton and Cline, 1998).

Several lines of evidence argue that NMDA receptors do play a specific role in the activity-dependent development of connections. First, reducing the expression and function of the R1 subunit of NMDA receptors in visual cortex with antisense DNA blocks ocular dominance plasticity (Roberts et al., 1998), similar to that obtained with infusion of D-APV into visual cortex (Bear et al., 1990) but without

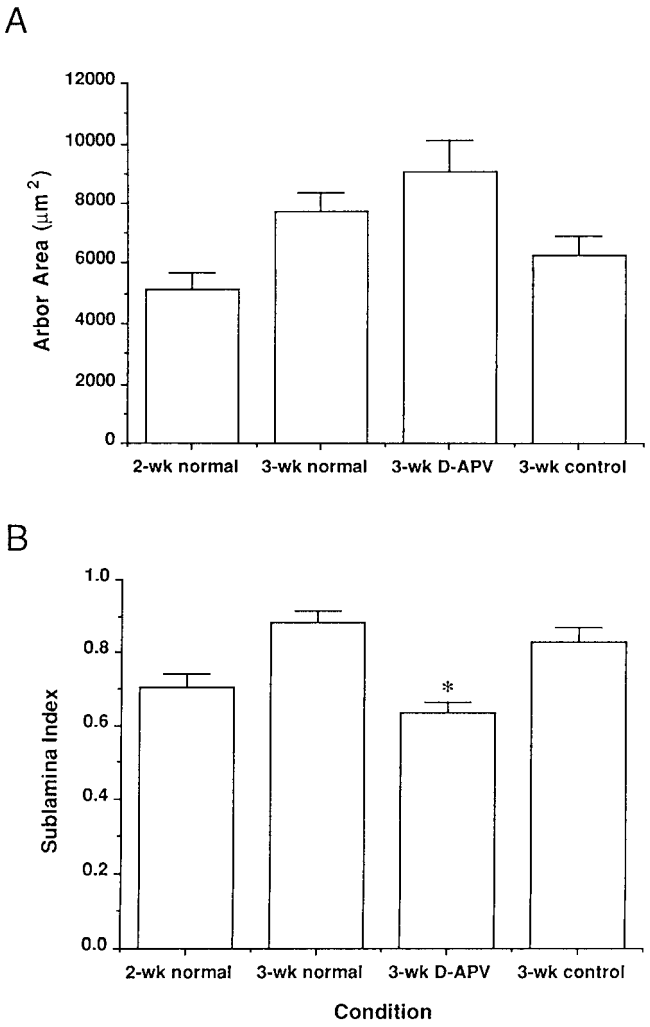

Fig. 14. Histograms showing measures of arbor area and degree of segregation of retinogeniculate axons. **A:** Terminal arbor areas of retinogeniculate axons in normal two-week-old (2-wk), normal three-week-old (3-wk), D-APV-treated 3-week-old, and drug-control three-week-old animals. Arbors in D-APV-treated animals are similar in area to three-week normal and drug-control axons. **B:** Histogram of "sublamina index," a measure to illustrate degree of segregation of axon arbors into the inner or outer half of an eye-specific lamina (for details, see text). A measure of 0.5 indicates complete lack of segregation; that is, arbors are placed equally in both halves of the lamina. A measure of 1.0 indicates total segregation to within an inner or outer half of a lamina. In normal two-week-old animals, most arbors are not segregated into sublaminae—the sublamina index indicates that axons are roughly midway in segregation. In normal and drug-control three-week-old animals, arbors are largely segregated within an eye-specific lamina, with a significantly higher sublamina index compared with two-week-old normal animals. In D-APV-treated animals, axon arbors are not segregated to an inner or outer half of the lamina and have a sublamina index significantly lower than normal three-week-old or drug-control animals (asterisk).

reducing the visual responses of cortical neurons. Second, in the retinofugal pathways, the effects of NMDA receptor blockade appear to be much more subtle than the effects of blocking all activity with TTX. Thus, the effect of NMDA receptor blockade on retinogeniculate axons (Hahm et al., 1991; present study) is mainly to alter arbor location and patterning rather than arbor size, whereas TTX (albeit with both pre- and postsynaptic blockade after intrathalamic infusion) alters arbor morphology drastically (Sretavan et al., 1988). In three-eyed frogs reared with NMDA receptor block of the tectum, retinotectal afferents have arbor areas similar to normal but reduced branch density (Cline and Constantine-Paton, 1990). In contrast, these afferents are abnormally large and widespread in frogs reared with TTX blockade of activity (Reh and Constantine-Paton, 1985).

It is important to note that signals that act downstream of NMDA receptors are being clarified in several developmental systems. Our results, whereby blockade of receptors on postsynaptic LGN cells alters presynaptic retinal arbors, indicate the existence of a mechanism in which the target influences the afferent to locate its arbor in a certain place. It is likely that a retrograde messenger reports postsynaptic activity to presynaptic terminals in the retinogeniculate pathway. Nitric oxide (NO) has been proposed as the retrograde messenger in this system. In the ferret LGN, levels of nicotinamide adenine dinucleotide phosphate-diaphorase (which colocalizes with NO synthase; NOS) exhibit developmental regulation, with a peak broadly coincident with the time period of sublaminar segregation during the third and fourth postnatal weeks (Cramer et al., 1995). Blockade of NOS during this period disrupts sublamination in a manner similar to that after NMDA receptor blockade (Cramer et al., 1996), indicating that NO acts downstream of NMDA receptors in mediating activity-dependent segregation of retinogeniculate afferents. More recently, additional signals in LGN neurons that rely on NMDA receptor activation and intracellular Ca^{2+} have been implicated. Levels of cyclic guanosine monophosphate (cGMP) in neurons of the ferret LGN are up-regulated during sublaminar segregation; these levels are increased by stimulation with NMDA and NO and are decreased by blockade of NOS (Leamey et al., 1998). Inhibiting soluble guanylyl cyclase/cGMP during the period of sublaminar segregation leads to their disruption. Similarly, calcineurin, a calcium/calmodulin-dependent protein phosphatase, has been postulated to be an important effector of NMDA receptor activity (Snyder and Sabatini, 1995). Calcineurin levels also are regulated developmentally in the ferret LGN (Ho-Pao et al., 1998), and blockers of calcineurin disrupt sublaminar segregation.

It is noteworthy that the formation of eye-specific layers during the first postnatal week does not require NMDA receptor activation (Smetters et al., 1994) or NO synthesis (Cramer et al., 1996). We have suggested elsewhere that activity-dependent pattern formation in the retinogeniculate pathway may implement at least two distinct biochemical mechanisms: one for eye-specific segregation and another for ON/OFF segregation (Cramer et al., 1998).

It is possible that blockade of NMDA receptors during ON/OFF sublamination affects retinogeniculate X and Y axons differently. It has been shown previously that retinogeniculate X and Y axons in cats have different responses to alterations in activity or removal of inputs (Garraghty and Sur, 1993). Manipulations late in development primarily affect arbor sizes: Blockade of retinal activity with intraocular injection of TTX or reducing activity with lid suture maintains X arbors at larger sizes and Y arbors at smaller sizes than normal, preventing their normal development (Sur et al., 1982, 1985). Manipulations early in development also affect arbor location: Removing one eye in cats at embryonic day 44 (E44; Garraghty et al., 1988) or

at E36 (Garraghty et al., 1998), when binocular afferents are intermixed in the LGN, leads to striking abnormalities in the position of Y axon arbors, whereas X arbors are affected less. Although X and Y axons were not identified separately by physiological recording in the present experiments, the hypothesis from the work summarized above is that the location of Y arbors would be much more susceptible to NMDA receptor blockade than the location of X arbors.

Axonal patterning and the dendritic development of LGN cells

Retinogeniculate lamination involves not only axonal segregation but also the formation of cell layers with the LGN. Normal development of geniculate lamination is dependent on the presence of retinal afferents from both eyes; without binocular afferents, neither cell layers nor interlaminar spaces form (Rakic, 1977; Brunso-Bechtold and Casagrande, 1981; Guillery et al., 1985). Removal of one eye early in development also disrupts the normal formation of laminae (Rakic, 1981; Brunso-Bechtold and Casagrande, 1983; Chalupa and Williams, 1984; Guillery et al., 1985). In the ferret LGN, lamination appears to be triggered by retinal afferents, in that cell layers begin to form only after the afferents have begun to segregate, even though completion of cell lamination is not contingent on completion of afferent segregation (Linden et al., 1981). The specific influence of retinal afferents on lamina formation is demonstrated in ferrets monocularly enucleated at birth: Whereas interlaminar zones between eye-specific laminae do not form in these animals, interleaflet spaces do form between sublaminar leaflets in the A and A1 laminae of the remaining eye (Guillery et al., 1985).

Dendrites of LGN cells develop progressively in arbor extent, branching, and the number and density of spines on a time course similar to that for the size and location of retinogeniculate axon arbors (Rocha and Sur, 1992, 1995). The regulation of dendritic morphology is also dependent on neuronal activity: LGN cells have increased spines after intrathalamic infusion of TTX in fetal cats (Dalva et al., 1994), and dendritic branching and spines on LGN cells are up-regulated when NMDA receptors are blocked during the third postnatal week in ferrets (Rocha and Sur, 1995). Thus, activity serves to coordinate the morphology of both retinogeniculate axons and LGN cells and the development of connections between the two.

ACKNOWLEDGMENTS

We thank Theresa Sullivan and Suzanne Kuffler for technical assistance and Ronald Langdon for his contributions. The axons in Figures 5, 6, and 12 are reprinted from Hahm et al. (1991) by permission from *Nature*, Macmillan Magazines Ltd. This work was supported by National Institutes of Health grants EY07023 and EY11512 to M.S.

LITERATURE CITED

Adams JC. 1981. Heavy metal intensification of DAB-based HRP reaction product. J Histochem Cytochem 29:775.

Archer S, Dubin M, Stark L. 1982. Abnormal retinogeniculate connectivity in the absence of action potentials. Science 217:743–745.

Arnett D. 1978. Statistical dependence between neighboring retinal ganglion cells in goldfish. Exp Brain Res 32:49–53.

Arnett D, Spraker T. 1981. Cross-correlation analysis of the maintained discharge of rabbit retinal ganglion cell. J Physiol (London) 317:29–47.

Bear MF, Kleinschmidt A, Gu Q, Singer W. 1990. Disruption of experience-dependent synaptic modifications in striate cortex by infusion of an NMDA receptor antagonist. J Neurosci 10:909–925.

Brunso-Bechtold JK, Casagrande VA. 1981. Effect of bilateral enucleation on the development of layers in the dorsal lateral geniculate nucleus. Neuroscience 6:2579–2586.

Brunso-Bechtold JK, Casagrande VA. 1983. Development of layers in the dorsal lateral geniculate nucleus in the tree shrew. In: Neff WD, editor. Contributions to sensory physiology, vol. 8. New York: Academic Press. p 41–77.

Bunt SM, Lund RD, Land PW. 1983. Prenatal development of the optic projection in albino and hooded rats. Dev Brain Res 6:149–168.

Campbell G, Shatz CJ. 1992. Synapses formed by identified retinogeniculate axons during the segregation of eye input. J Neurosci 12:1847–1858.

Chalupa L, Williams RW. 1984. Organization of the cat's lateral geniculate nucleus following interruption of prenatal binocular competition. Hum Neurobiol 3:103–107.

Cline HT, Constantine-Paton M. 1989. NMDA receptor antagonists disrupt the retinotectal topographic map. Neuron 3:413–426.

Cline HT, Constantine-Paton M. 1990. NMDA receptor agonist and antagonists alter retinal ganglion cell arbor structure in the developing frog retinotectal projection. J Neurosci 10:1197–1216.

Cline HT, Debski EA, Constantine-Paton M. 1987. N-methyl-D-aspartate receptor antagonist desegregates eye-specific stripes. Proc Natl Acad Sci USA 84:4342–4345.

Constantine-Paton M, Cline HT. 1998. LTP and activity-dependent synaptogenesis: the more alike they are, the more different they become. Curr Opin Neurobiol 8:139–148.

Cramer KS, Sur M. 1995. Activity-dependent remodeling of connections in the mammalian visual system. Curr Opin Neurobiol 5:106–111.

Cramer KS, Sur M. 1997. Blockade of afferent impulse activity disrupts on/off sublamination in the ferret lateral geniculate nucleus. Dev Brain Res 98:287–290.

Cramer KS, Moore CI, Sur M. 1995. Transient expression of NADPH-diaphorase in the lateral geniculate nucleus of the ferret during early postnatal development. J Comp Neurol 353:306–316.

Cramer KS, Angelucci A, Hahm J, Bogdanov MB, Sur M. 1996. A role for nitric oxide in the development of the ferret retinogeniculate projection. J Neurosci 16:7995–8004.

Cramer KS, Leamey CA, Sur M. 1998. Nitric oxide as a signaling molecule in visual system development. Progr Brain Res 118:101–114.

Cucchiaro J, Guillery RW. 1984. The development of the retinogeniculate pathways in normal and albino ferrets. Proc R Soc London 223:1141–1164.

Dalva MB, Ghosh A, Shatz CJ. 1994. Independent control of dendritic and axonal form in the developing lateral geniculate nucleus. J Neurosci 14:3588–3602.

Dubin MW, Stark LA, Archer SM. 1986. A role for action-potential activity in the development of neuronal connections in the kitten retinogeniculate pathway. J Neurosci 6:1021–1036.

Esguerra M, Kwon YH, Sur M. 1992. Retinogeniculate EPSPs recorded intracellularly in the ferret lateral geniculate nucleus in vitro: role of NMDA receptors. Visual Neurosci 8:545–555.

Fox K, Sato H, Daw N. 1989. The location and function of NMDA receptors in cat and kitten visual cortex. J Neurosci 9:2443–2454.

Galli L, Maffei L. 1988. Spontaneous impulse activity of rat retinal ganglion cells in prenatal life. Science 242:90–91.

Garraghty PE, Sur M. 1993. Factors influencing the development of retinal axon arbors in the cat's lateral geniculate nucleus. Physiol Rev 73:529–545.

Garraghty PE, Shatz CJ, Sretavan DW, Sur M. 1988. Axon arbors of X and Y retinal ganglion cells are differentially affected by prenatal disruption of binocular inputs. Proc Natl Acad Sci USA 85:7361–7365.

Garraghty PE, Roe A, Sur M. 1998. Specification of retinogeniculate X and Y axon arbors in cats: fundamental differences in developmental programs. Dev Brain Res 107:227–231.

Greiner JV, Weidman TA. 1981. Histogenesis of the ferret retina. Exp Eye Res 33:315–322.

Guillery RW, Lamantia AS, Robson JS, Huang K. 1985. The influence of retinal afferents upon the development of layers in the dorsal lateral geniculate nucleus of mustelids. J Neurosci 5:1370–1379.

Hahm J, Langdon RB, Sur M. 1991. Disruption of retinogeniculate afferent segregation by antagonists to NMDA receptors. Nature 351:568–570.

Hartveit E, Heggelund P. 1990. Neurotransmitter receptors mediating

excitatory input to cells in the cat lateral geniculate nucleus. II. Non-lagged cells. J Neurophysiol 63:1361–1372.

Heggelund P, Hartveit E. 1990. Neurotransmitter receptors mediating excitatory input to cells in the cat lateral geniculate nucleus. I. Lagged cells. J Neurophysiol 63:1347–1360.

Ho-Pao CL, Leamey CA, Sur M. 1998. Calcineurin expression in lateral geniculate nucleus (LGN) of developing ferrets. Soc Neurosci Abstr 24:63.

Hohnke CD, Sur M. 1999. Stable properties of spontaneous EPSCs and miniature retinal EPSCs during the development of on/off sublamination in the ferret lateral geniculate nucleus. J Neurosci 19:236–247.

Hutchins JB, Casagrande VA. 1990. Development of the lateral geniculate nucleus: interactions between retinal afferent, cytoarchitectonic, and glial cell process lamination in ferrets and tree shrews. J Comp Neurol 298:113–128.

Kleinschmidt A, Bear MF, Singer W. 1987. Blockade of NMDA receptors disrupts experience-dependent plasticity of kitten striate cortex. Science 238:355–358.

Kwon YH, Esguerra M, Sur M. 1991. NMDA and non-NMDA receptors mediate visual responses of neurons in the cat's lateral geniculate nucleus. J Neurophysiol 66:414–428.

Leamey CA, Ho-Pao CL, Sur M. 1998. Downstream signalling of the NMDA receptor/nitric oxide pathway during on/off sublamina formation in the ferret LGN: a role for gualynyl cyclase? Soc Neurosci Abstr 24:1051.

LeVay S, McConnell SK. 1982. On and off layers in the lateral geniculate nucleus of the mink. Nature 300:350–351.

Linden DC, Guillery RW, Cucchiaro J. 1981. The dorsal lateral geniculate nucleus of the normal ferret and its postnatal development. J Comp Neurol 203:189–211.

Mason CA. 1982. Development of terminal arbors of retino-geniculate axons in the kitten: I. light microscopical observations. Neuroscience 7:541–559.

Meister M, Wong RO, Baylor DA, Shatz CJ. 1991. Synchronous bursts of action potentials in ganglion cells of the developing mammalian retina. Science 252:939–943.

Mesulam M-M. 1982. Tracing neural connections with horseradish peroxidase. IBRO handbook series: methods in the neurosciences. New York: John Wiley and Sons.

Miller KD, Chapman B, Stryker MP. 1989. Visual responses in adult cat visual cortex depend on N-methyl-D-aspartate receptors. Proc Natl Acad Sci USA 86:5183–5187.

Mooney R, Madison DV, Shatz CJ. 1993. Enhancement of transmission at the developing retinogeniculate synapse. Neuron 10:815–825.

Movshon JA, Van Sluyters RC. 1981. Visual neural development. Annu Rev Psychol 32:477–522.

Penn AA, Riquelme PA, Feller MB, Shatz CJ. 1998. Competition in retinogeniculate patterning driven by spontaneous activity. Science 279:2108–2112.

Rakic P. 1977. Prenatal development of the visual system in rhesus monkey. Phil Trans R Soc London 278:245–260.

Rakic P. 1979. Genesis of visual connections in the rhesus monkey. In: Freeman RD, editor. Developmental neurobiology of vision. New York: Plenum Press. p 249–276.

Rakic P. 1981. Development of visual centers in the primate brain depends on binocular competition before birth. Science 214:928–931.

Ramoa AS, McCormick DA. 1994. Developmental changes in electrophysiological properties of LGNd neurons during reorganization of retinogeniculate connections. J Neurosci 14:2089–2097.

Reese, BE. 1987. The position of the crossed and uncrossed optic axons, and the non-optic axons, in the optic tract of the rat. Neuroscience 22:1025–1039.

Reh TA, Constantine-Paton M. 1985. Eye-specific segregation requires neural activity in the three-eyed *Rana pipiens*. J Neurosci 5:1132–1143.

Roberts EB, Meredith MA, Ramoa AS. 1998. Suppression of NMDA receptor function using antisense DNA blocks ocular dominance plasticity while preserving visual responses. J Neurophysiol 80:1021–1032.

Rocha M, Sur M. 1992. Dendritic development of LGN cells during laminar and sublaminar segregation. Soc Neurosci Abstr 18:1310.

Rocha M, Sur M. 1995. Rapid acquisition of dendritic spines by visual thalamic neurons after blockade of N-methyl-D-aspartate receptors. Proc Natl Acad Sci USA 92:8026–8030.

Roe AW, Garraghty PE, Sur M. 1989. Terminal arbors of single on-center and off-center X and Y retinal ganglion cell axons within the ferret's lateral geniculate nucleus. J Comp Neurol 288:208–242.

Scherer WJ, Udin SB. 1989. N-methyl-D-aspartate antagonists prevent interaction of binocular maps in *Xenopus* tectum. J Neurosci 9:3837–3843.

Shatz CJ. 1983. The prenatal development of the cat's retinogeniculate pathways. J Neurosci 3:482–499.

Shatz CJ, Kirkwood PA. 1984. Prenatal development of functional connections in the cat's retinogeniculate pathway. J Neurosci 4:1378–1397.

Shatz CJ, Stryker MP. 1988. Prenatal tetrodotoxin infusion blocks segregation of retinogeniculate afferents. Science 242:87–89.

Sherman SM. 1985. Development of retinal projections to the cat's lateral geniculate nucleus. Trends Neurosci 8:350–355.

Sherman SM, Spear PD. 1982. Organization of visual pathways in normal and visually deprived cats. Physiol Rev 62:738–855.

Sillito AM, Murphy PC, Salt TE. 1990a. The contribution of the non-N-methyl-D-aspartate group of excitatory amino acid receptors to retinogeniculate transmission in the cat. Neuroscience 34:273–280.

Sillito AM, Murphy PC, Salt TE, Moody CI. 1990b. Dependence of retinogeniculate transmission in cat on NMDA receptors. J Neurophysiol 63:347–355.

Smetters DK, Hahm J, Sur M. 1994. An N-methyl-D-aspartate receptor antagonist does not prevent eye-specific segregation in the ferret retinogeniculate pathway. Brain Res 658:168–178.

Snyder SH, Sabatini DM. 1995. Immunophilins and the nervous system. Nat Med 1:32–37.

Sretavan DW, Shatz CJ. 1986. Prenatal development of retinal ganglion cell axons: segregation into eye-specific geniculate layers from the intermixed state. J Neurosci 6:234–251.

Sretavan DW, Shatz CJ, Stryker MP. 1988. Modification of retinal ganglion cell axon morphology by prenatal infusion of tetrodotoxin. Nature 336:468–471.

Stryker MP, Harris W. 1986. Binocular impulse blockade prevents the formation of ocular dominance columns in cat visual cortex. J Neurosci 6:2117–2133.

Stryker MP, Zahs KR. 1983. On and off sublaminae in the lateral geniculate nucleus of the ferret. J Neurosci 3:1943–1951.

Sur M, Humphrey AL, Sherman SM. 1982. Monocular deprivation affects X- and Y-cell retinogeniculate terminations in cats. Nature 300:183–185.

Sur M, Garraghty PE, Stryker MP. 1985. Morphology of physiologically identified retinogeniculate axons in cats following blockade of retinal impulse activity. Soc Neurosci Abstr 11:805.

White CA, Sur M. 1992. Membrane and synaptic properties of developing lateral geniculate nucleus neurons during retinogeniculate axon segregation. Proc Natl Acad Sci USA 89:9850–9854.

Wong ROL, Oakley DM. 1996. Changing patterns of spontaneous bursting activity of on and off retinal ganglion cells during development. Neuron 16:1087–1095.

Wong ROL, Meister M, Shatz CJ. 993. Transient period of correlated bursting activity during development of the mammalian retina. Neuron 11:923–938.